A

M.Sc. Project Thesis

On

Stimuli Responsive Hydrogen Bonded Capsule Formation through Dynamic Self-Assembly for Guest/Drug Transport

Submitted in partial fulfillment of requirement for the award of degree of

Master of Science

In

Chemistry

Submitted by

Akshita

Roll No.-301602004

Supervisor

Dr. Ashutosh Sharan Singh

and

Dr. Vijay Luxami

Submitted To

School of Chemistry and Biochemistry

THAPAR INSTITUTE OF ENGINEERING AND TECHNOLOGY

PATIALA – 147004 (PUNJAB)

Dedicated To My Family

Certificate

I hereby declare that the thesis enititled ***"Stimuli Responsive Hydrogen Bonded Capsule Formation through Dynamic Self-Assembly for Guest/Drug Transport."*** Is an authentic record of my work carried out as requirements for the award of degree of Master's of Science in Chemistry at Thapar Institute of Engineering and Technology, Patiala under the supervision of Dr. Ashutosh Sharan Singh, Associate Professor at Chandigarh University and Dr. Vijay Luxami,, Associate Professor at School of Chemistry and Biochemistry, TIET during January 2018 to June 2018. No part of matter embodied in this report has been submitted to any other university for the award of any degree.

Akshita

Date 25-07-2018 AKSHITA

It is certified that the above statement that the above statement made by student is correct to my knowledge and belief.

Signature of Report Supervisor

Date : 25-07-2018

Signature of Report Supervisor

Date: 25-07-2018

Candidate's Declaration

I hereby declare that the thesis entitled "**Stimuli Responsive Hydrogen Bonded Capsule Formation through Dynamic Self-Assembly for Guest/Drug Transport"** is an authentic record of my work carried out in partial fulfilment of the requirements for the award of the degree of Master of Science in Chemistry at Thapar Institute of Engineering and technology, Patiala under the supervision of Dr. Ashutosh Sharan Singh, Associate Professor, Chandigarh University, Chandigarh and Dr. Vijay Luxami, Assistant Professor, School of Chemistry and Biochemistry(SCBC), Thapar Institute of Engineering & Technology (TIET), Patiala during January 2018 to June 2018. No part of the matter embodied in this report has been submitted to any other university or institute for the award of any degree.

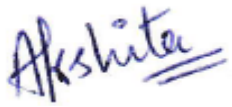

Signature of Student

ACKNOWLEDGEMENT

I would like to express my deep and sincere gratitude to my supervisors **Dr. Ashutosh Sharan Singh** and **Dr. Vijay Luxami**. Their wide knowledge and logical way of thinking have been a great value for me. Their understanding, encouragement, detailed and constructive comments and personal guidance have provided a good basis for present report. In addition, they were always accessible and willing to help their students with their research. I believe that the kind of training I have gone under their guidance will help me throughout my future.

I would also like to acknowledge Prof. Prakash Gopalan, Director TIET, Patiala, India and Head of School of Chemistry and Biochemistry Dr. Amjad Ali for helping me in smooth conduction of my research by providing the best infrastructure and instrumental facilities.

I express my appreciation to SAI Labs for their unceasing service and availability.

I also acknowledge the support of Hemant sir, the laboratory staff and Mayank sir who helped me in every possible way.

I sincerely thank my lab senior Richa Bansal, Gulshan Kumar, Ruhi Mehta, Aastha Palta, Iqubal Singh, Sudesh Rani, Dinesh Singla for teaching me lab techniques, collection of various experimental data and fruitful discussions.

I wish to extend my warmest thanks to all my friends at Thapar Institute of Engineering and Technology, Patiala, India.

My deepest gratitude to God and my family for their unflagging love and support throughout my life.

ABSTRACT

Discrete confined cavity pore of molecular capsule is of paramount significance for numerous purposes. If capsule assembled through weak non-covalent interaction(s) like hydrogen bonding then system can be made responsive for reversible binding/encapsulation of guest molecule.

However, more often cavity tends to collapse, especially if such cavity/pore is created by π–extended purely organic moieties. The situation becomes even more complicated in the solution-state especially with flexible bridging of receptors, if it can undergo various possible conformation because π•••π interactions typically dominate in the self-assembly process and surrounding environment also plays a critical role in the molecular assembly.

We attempt to short out this problem by implementing self-sorting and bio-inspired mutual induce-fit process (rarely observed in an artificial system). Self-sorting provides ample opportunity to design and simplify the synthetic scheme through multi-component assembly. On the other hand mutual induce-fit provides insight to make control of such dynamic system. The key feature of selfsorted assembly is high fidelity and feasibility to achieve the target in excellent yield that overcome traditional synthetic methodology.

Introduction

Molecular container possessing cavity is of paramount significance to study the behavior of encapsulated guest(s) molecule. The cavity inside container provides constrain environment and so encapsulated guest molecule is away from surrounding environments like solvent interaction, pH of surrounding medium and act as nanoreactor.[1]Several types of molecular container explored till now (Fig. 1) like crown ether[2], cyclophanes[3], cyclodextrins[4], spherand[2], cavitands[2], calixarenes[5], cucurbit[n]urils[6], porphyrins[7], zeolites[8] and metal-organic frameworks (MOFs)[9] etc. The behavior of encapsulated guest molecule in a confined cavity differ vastly from bulk medium like change in pK_a value[10], specificity, and packing arrangement[11] etc. These properties resemble biological system where biochemical processes like catalysis occur in confined space with change in pK_a value[12].

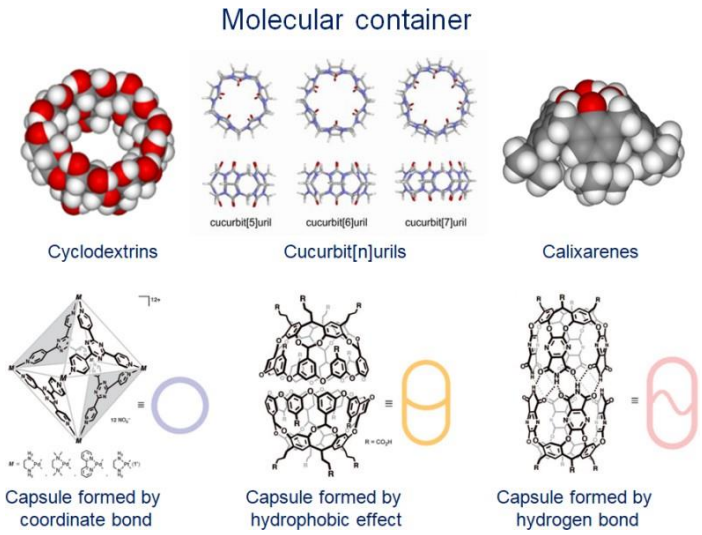

Fig. 1 Examples of commonly used molecular container with different shape and size.

1.1 Molecular Capsule

Molecular capsule is an important and well explored member of supramolecular family.[13] It provides discrete 3-dimensional interior cavity. Discrete cavity playing important role for study the behavior of encapsulated guest as well as the mechanism of chemical transformation. In literature, various types (shape and size) of molecular capsule possessing discrete cavity has been explored and utilized for various purposes like catalysis[14], encapsulation of guest[15], isomersiation[16], stabilization of explosive[17], stabilization of unstable species[18], exceptional

reactivity[19], activation of drug[10] etc. Molecular capsule (Fig. 1) may be synthesized by hydrogen-bonding interactions[20], ionic interactions[21], hydrophobic interactions[22], metal co-ordination bond[23].

1.2 Hydrogen bonded capsule

Hydrogen-bond is comparatively much weaker (~5 kJ/mol) than electrostatic interaction (20 kJ/mol), coordinate bond or even hydrophobic interactions (~40 kJ/mol). However, capsule formed by same unit, homomeric capsule or different unit, heteromeric capsule through a series of complementary hydrogen bond having sufficient life-time to study on NMR time scale.[20e] Hydrogen-bonded capsule is having some unique characteristic features like: 1) complimentary donor-acceptor binding motifs can be taken by judicial choice. Its strength can be altered/manipulated, 2) H-bonded capsule is having short life-time[24] that can be increased by incorporation of suitable solvent molecule[24] and 3) H-bonds are very weak (~5 kJ/mol) and so it may be tuned with external stimuli to form responsive capsule which would be highly useful for guest/drug transport process[25]. Numerous examples of H-bonded capsule are reported in literature which may be homomeric or heteromeric (Fig 3-10).

1.3 Literature on hydrogen-bonded capsule

Hydrogen bond (**A-H•••B**, where '**A**' and '**B**' are electronegative atoms which may be same or different) is a directional bond and its strength depends upon distance and angle between proton attached to electronegative atom ('**A**') and neighboring electronegative atom (here '**B**'). Shorter the distance, stronger will be the bond. If angle between **A-H•••B** is 180°, H-bond will be stronger. Based upon complementary binding motifs and judicial choice of organic moiety, H-bonded capsule of different size and shapes have been explored in literature for various purposes.

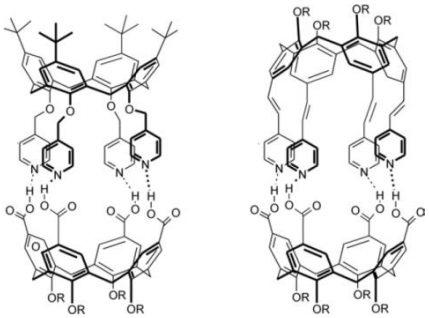

Fig. 2 Hydrogen bonded heterodimeric capsule with cylindrical cavity.

Hydrogen-bonded homomeric/heteromeric capsules of different size and shapes

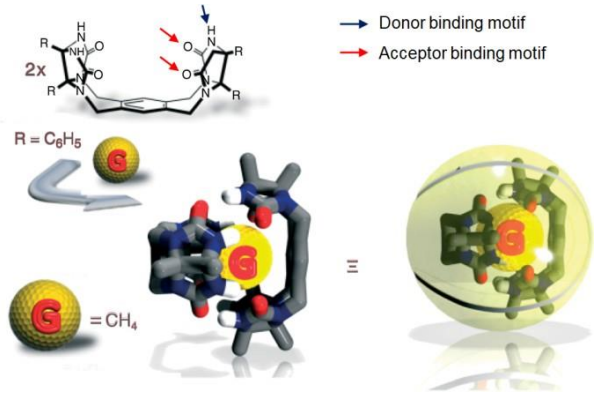

Fig. 3 Homomeric dimer like tenis ball encapsulating methane molecule.

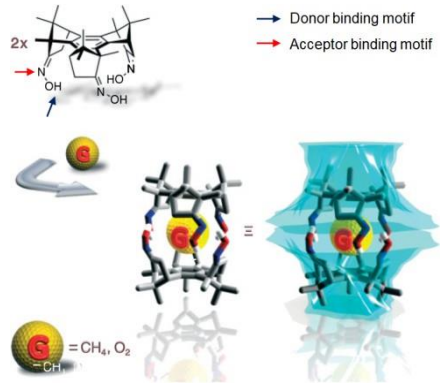

Fig. 4 Homomeric dimer of benzocyclotrimer tris-oxime for methane and oxygen hosting.

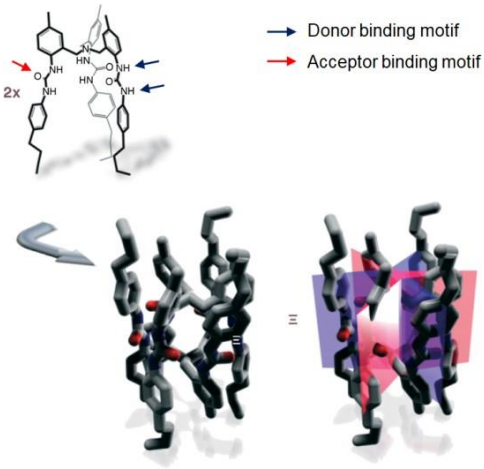

Fig. 5 Homomeric dimer of urea-based tris(2-ureidobenzylamine), forming H-bonded capsule.

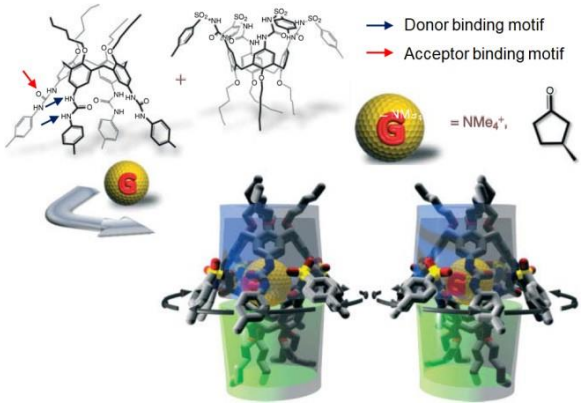

Fig. 6 Heteromeric dimer of tetraarylurea and tetratosylurea calix[4]arene, forming chiral capsule.

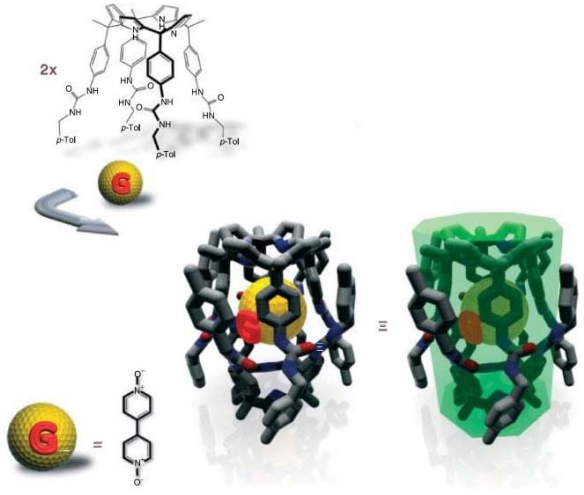

Fig. 7 Homomeric dimer of calix[4]pyrrole, forming H-bonded capsule for anionic guest.

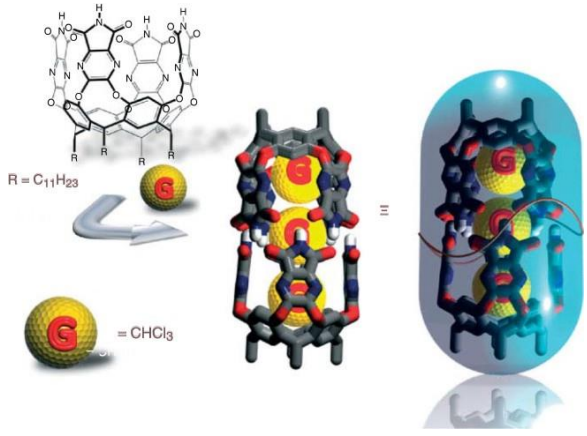

Fig. 8 Cylindrical homodimeric capsule that can accomodate up to three guest molecules.

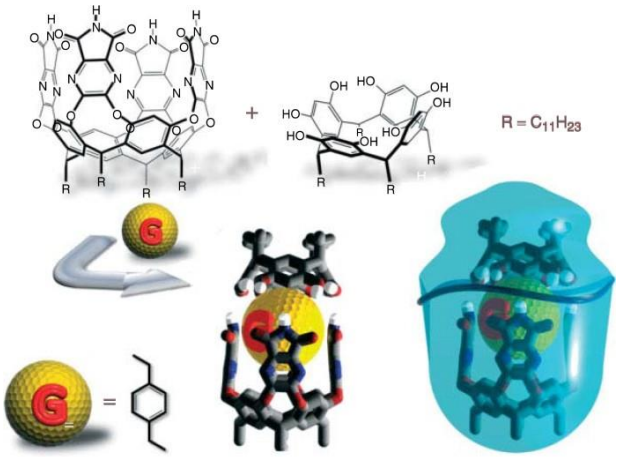

Fig. 9 Heterodimeric capsule between tetraminde cavitand and resorcin[4]arene with suitable guest.

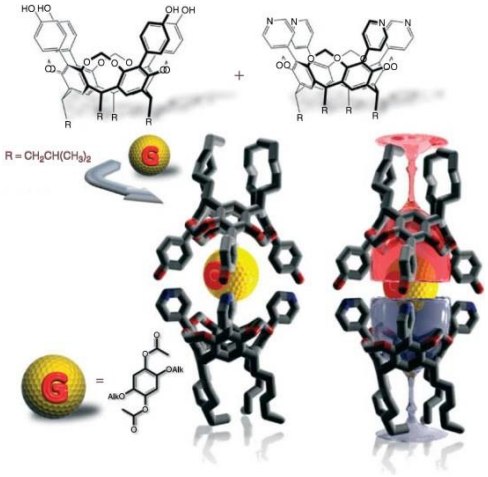

Fig. 10 Heterodimeric H-bonded capsule showing slow spinning for encapsulated guest.

1.4 Significance of hydrogen-bonded capsule

Hydrogen bond is sensitive to external factor like pH, polarity of solvent, temperature etc. and so capsule based upon hydrogen bonding can be reversibly transformed between monomeric unit and hydrogen bonded capsule. Interior cavity of capsule act as nano-reactor and help to isolate the product after chemical transformation with great ease. Especially for chemical transformations where shape of product changes after catalysis, binding affinity of product will change and as a result turn over number will increase. Therefore, for chemical transformation (catalysis) and release of encapsulated guest (guest/drug delivery) hydrogen bonded capsules are of better choice.

2. Research gap in study

The reported examples of molecular capsules were static and there were no control for reversible transformation of monomer to capsule formation for efficient practical applications like stimuli responsive guest/drug release. Although, pH dependent reversible transformation between monomer to capsule formation is known[26] yet it has been observed that after couple of cycle (between monomer and capsule form) some uncharacterized by-product was forming. Therefore, there were desperate need of a system which can assemble through H-bond to form capsule in response to suitable external stimuli. Recently, an exceptional example were reported[25,27] by Singh et al. where solvent polarity dependent reversible capsule formed and no by-product observed after couple of cyclic transformation between monomer and capsule form (Fig. 11).

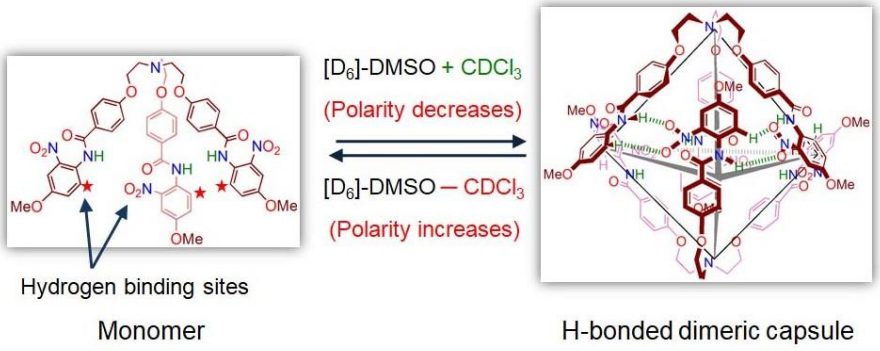

Fig. 11 Solvent polarity dependent reversible assembly to form H-bonded capsule.

2.1 Drawback in hydrogen bonded capsule

The major drawback with hydrogen-bonded capsule is that the cavity size of the capsule is restricted up to certain limit[24] as the energy of hydrogen bonding is quite low i.e. 5 kJ/mole also strength of H-bonding depends on two factors i.e. distance between the binding motifs and angular dependence. If the angle between donor and accepter moiety is 180° then in this case H-bonding is strongest and vice-versa.

Moreover, cavity tends to collapse, especially if such cavity/pore is created by π–extended purely organic moieties in order to increase the cavity size. The situation becomes even more complicated in the solution-state especially with flexible bridging of receptors, if it can undergo various possible conformation because π•••π interactions typically dominate in the self-assembly process and surrounding environment also plays a critical role in the molecular assembly.

2.2 Possibility of solving the drawback through mutual induced fit

We attempt to short out this problem by implementing bio-inspired mutual induce-fit[28] process (rarely observed in an artificial system).

2.3 Mutual induced fit

Mutual Induce fit is a natural phenomenon mainly observed in biological system and first proposed by Koshland[29]. It is advanced form of "Key-lock principle" where Fischer explains that substrate (starting compound of reaction) can be assumed as “key” and enzymes as “lock” and only specific substrate (key) that can perfectly fit into enzymes (lock), catalysis will occur otherwise that substrate cannot be catalyzed by that particular enzyme. One hidden part of “key-

Lock principle' was rigidity, and if substrate (starting compound of reaction) is not rigid to fit into particular enzyme, catalytic process cannot take place. On the other side, in mutual induce fit the substrate as well as the enzyme sites are flexible (Fig. 12). Due to flexibility of the recognition sites, they mutually induce the organization of each other so that the two biomolecules interact strongly and with high specificity and catalytic process occurs.

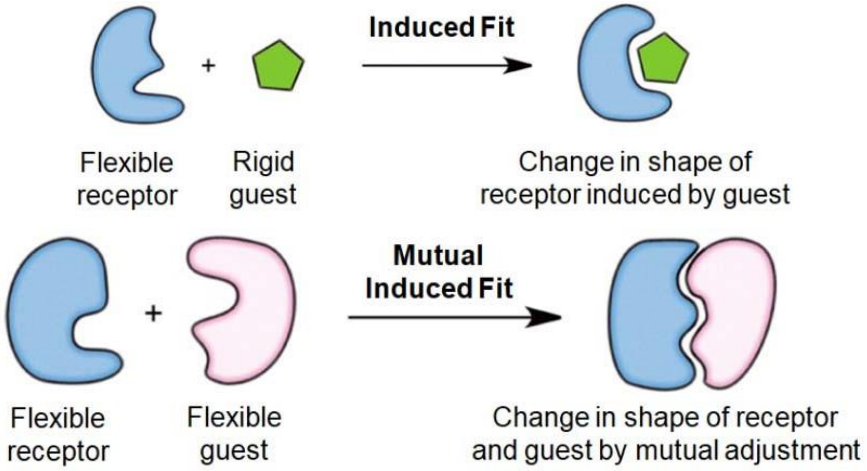

Fig. 12 Schematic representation of "Induced fit" and "Mutual induce fit".

Mutual induce-fit is an important and widely recognized phenomenon in biological systems[29] for enzymatic catalysis[30], peptide bond formation[31] and protein synthesis[32] etc. with high efficacy and specificity. The key feature in this phenomenon is reorganization of flexible components to optimize the final conformation. However, to mimic such processes in an artificial system is challenging and hence rare. Moreover, mimicking such biochemical phenomenon, through neutral non-covalent interactions, with purely organic acyclic flexible component(s) is till date unexplored.

2.4 Literature on mutual induced-fit

In a recently reported system, a flexible calix[4]arene is enclathrated in a dynamic self-assembled host and both molecules adopt specific three dimensional structures[28b].

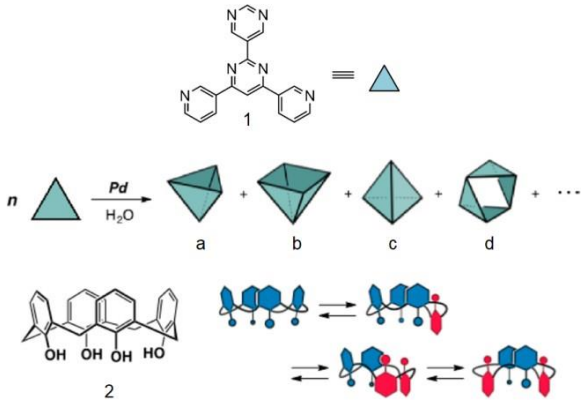

Fig. 13 Structure of ligand **1** (*top*). Cartoon representations of potential dynamic host library from ligand **1** (*middle*) and (en)Pd(NO_3)$_2$. Structure of calix[4]arene **2** and its conformational isomers.

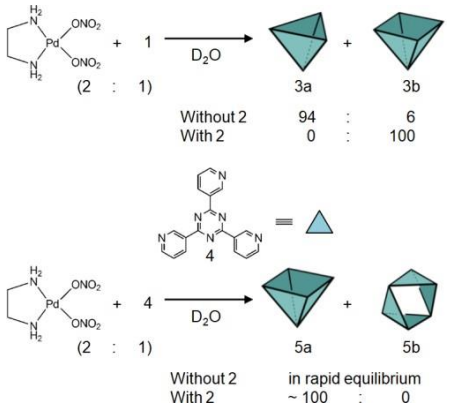

Fig. 14 Formation of **3a,b** (*top*) in the presence of **1** and structure of ligand **4** (*middle*) and formation of **5a,b** in the presence of **4**.

2.5 Objective: H-bonded capsule formation through mutual induced fit

In the present project, we have chosen two flexible ligand (one N-bridged tripodal ligand, Fig. 15 and another triazene moiety based tripodal ligand, Fig. 16) that can exist independently in a number of possible confirmation. The design of triazene core ligand is based upon following facts: (i) Triazene core was chosen because of its associated driving-force, through anion•••π and C-H•••π interaction to facilitate guest encapsulation,

(ii) the reactivity of two unsymmetrical formyl group of each arm will be biased towards aliphatic and aromatic amine, respectively. At room temperature, aliphatic amine (benzylamine) will prefer to react with *ortho*-substituted formyl group (with respect to alkoxy group) and aromatic amine (2-nitroaniline) will prefer to react with *para*-substituted formyl group. We speculate that if aromatic ring of benzylamine can be zipped symmetrically then resulting entity will come in cone-shape conformation and will behave like previously used receptor[27] with comparatively large cavity size.

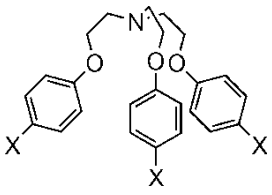

Fig. 15 N-bridged flexible receptor

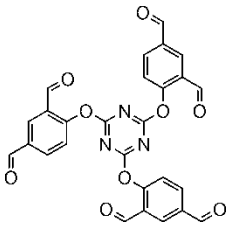

Fig. 16 Triazene core based ligand.

Experimental Section

Synthesis of receptor 1

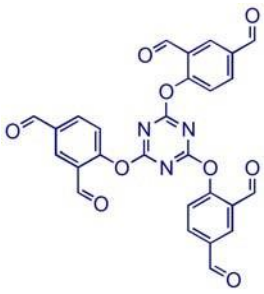

To 4-formylsalicyldehyde (1.831 g; 12.20 mmol) in 30 mL of dry benzene, anhydrous Na_2CO_3 (2.585 g; 24.39 mmol) was added and mixture suspension was allowed to stirr at room temperature for 15 min. Cyanuric chloride (0.75 g; 4.067mmol) was added to above suspension and mixture was allowed to reflux for 12 h. Benzene was removed under reduced pressure and crude product was extracted with ethyl acetate (100 mL x 2) and organic layer was washed with saturated sodium chloride solution. The organic layer was dried over anhydrous Na_2SO_4 and ethyl acetate was removed under reduced pressure. The crude product was later purified by column chromatography with ethyl acetate/hexane mixture solution to get required product as creamy yellow solid (0.984 g, yield ~ 46%).

^{1}H NMR (400 MHz, DMSO-[d_6]) δ = 11.78 (s, 1H), 10.33 (s, 1H), 9.88 (s, 1H), 8.20 (d, *J* = 2.1, 1H), 8.01 (dd, *J* = 8.6, 2.2, 1H), 7.16 (d, *J* = 8.6, 1H); **^{13}C NMR** (100 MHz, DMSO-[d_6]) δ = 191.05, 190.08, 165.44, 135.68, 132.01, 128.38, 122.55, 118.21; **HRESI mass spectrum** for $[M+H]^+$: m/z calcd 526.0881 found 526.0876; **IR**: 1666.60 and 1689.21 cm^{-1} (for >C=O).

General procedure for preparation of adducts 2, 4a-b, 5' and receptors 5a & 5b:

All adducts were prepared *in-situ* in DMSO-[d_6] solution of receptor **1** at room temperature.

Three parallel experiments were carried out at three different concentrations (100 mM, 25 mM and 1.56 mM) to check efficacy of induce-fit. To prepare adduct **2** ([**2**] = 100 mM), receptor **1** (21 mg, 0.04 mmol) was dissolved in 0.4 mL of DMSO-[d_6] and then benzylamine (3 equivalents, 13.11 µL, 0.12 mmol) was added to get mustard oil color solution of adduct **2**. To prepare adduct **4X** (**X**, depends upon *para*-substitution of aromatic ring of N-bridged receptors, like X = -NO_2(**4a**), and -F(**4b**), respectively), 3 equivalents of corresponding N-bridged receptor (**3a-b**) was added to adduct **2** and mixture suspension was sonicated for 10 min at room temperature to get transparent solution. Receptors **5a** and **5b** were prepared by adding 3 equivalents of 2-nitroaniline to DMSO-[d_6] solution of the adduct **4a** and **4b**, respectively at room temperature.

Adduct 2:

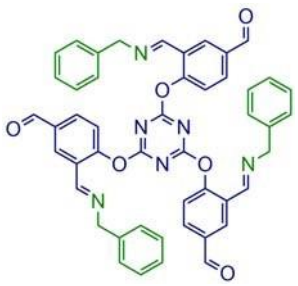

^{1}H NMR (400 MHz, DMSO-[d_6]) δ = 9.75 (s, 1H), 8.82 (s, 1H), 8.78 (s, 1H), 8.40 (s, 1H), 8.01 (d, *J* = 2.1, 1H), 7.95 (dd, *J* = 8.6, 1.1, 1H), 7.88 (d, *J* = 1.9, 1H), 7.80 (d, *J* = 2.1, 1H), 7.78 (d, *J* = 2.0, 1H), 7.76 (d, *J* = 2.0, 1H), 7.42 – 7.32 (m, 12H), 7.01 (dd, *J* = 8.5, 0.9, 2H), 6.91 (d, *J* = 8.6,1H), 6.84 (d, *J* = 8.8, 1H), 6.61 (ddd, *J* = 8.3, 7.0, 1.1, 1H), 4.87 (s, 2H) 4.82 (s, 1H), 4.77 (s, 1H), 4.76 (s, 1H), 4.73 (s,1H). IR: 163.79 cm^{-1} (>C=O)

Adduct 5':

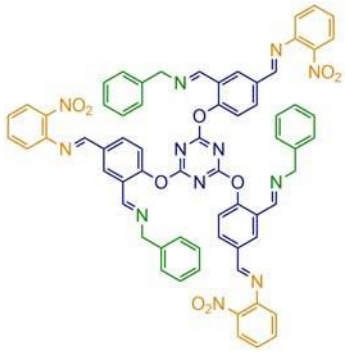

^{1}H NMR (400 MHz, DMSO-[d_6]) δ = 9.75 (s, 1H), 8.82 (s, 1H), 8.78 (s, 1H), 8.40 (s, 1H), 8.01 (d, *J*=1.8, 1H), 7.95 (d, *J*=8.5, 1H), 7.88 (d, *J*=1.4, 1H), 7.78 (td, *J*=9.1, 2.0, 2H), 7.43 – 7.28 (m, 14H), 7.01 (d, *J*=8.3, 1H), 6.91 (d, *J*=8.4, 1H), 6.84 (d, *J*=8.8, 1H), 6.61 (t, *J*=8.1, 1H), 4.87 (s, 2H), 4.82 (s, 1H), 4.76 (s, 1H), 4.73 (s, 1H), 1.83 (s, 2H), 1.70 (s, 5H); **^{13}C NMR** (100 MHz, DMSO-[d_6]) δ = 189.85 (s), 172.20 (s), 171.76 (s), 166.40 (s), 166.33 (s), 166.20 (s), 164.11 (s), 160.40 (s), 146.12 (s), 146.09 (s), 139.80 (s), 139.78 (s), 138.17 (s), 137.85 (s), 137.51 (s), 137.20 (s), 137.15 (s), 135.62 (s), 135.57 (s), 133.15 (s), 132.06 (s), 132.01 (s), 130.37 (s), 130.23 (s), 128.67 (s), 128.56 (s), 128.24 (s), 127.84 (s), 127.79 (s), 127.74 (s), 127.62 (s), 127.58 (s), 127.24 (s), 126.63 (s), 125.73 (s), 125.51 (s), 125.29 (s), 120.40 (s), 120.18 (s), 119.10 (s), 118.10 (s), 118.06 (s), 117.53 (s), 116.67 (s), 116.49 (s), 115.42 (s), 63.73 (s), 61.09 (s), 58.44 (s), 58.20 (s), 37.04 (s), 27.51 (s). **HRESI mass spectrum** for [**5'•H_2O**]$^+$: found *m/z* 1170.6208, calcd. *m/z* 1170.3773)

Adduct 4a:

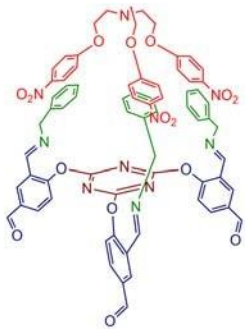

^{1}H NMR (400 MHz, DMSO-[d_6])) δ = 10.28 (s, 1H), 10.25 (s, 1H), 9.81 (s, 1H), 9.71 (s, 11H), 8.78 (s, 10H), 8.73 (s, 1H), 8.39 (s, 1H), 8.36 (s, 1H), 8.13 (d, *J*=2.2, 1H), 8.09 (d, *J*=9.2, 27H), 7.96 (d, *J*=2.1, 11H), 7.94 (d, *J*=2.2, 1H), 7.92 (d, *J*=2.2, 1H), 7.84 (d, *J*=2.0, 1H), 7.76 (d, *J*=2.1, 5H), 7.74 (d, *J*=2.1, 6H), 7.72 (d, *J*=2.1, 1H), 7.35 (d, *J*=1.7, 16H), 7.3(s,24H),7.31

(d, *J*=1.5, 4H), 7.28 (t, *J*=5.4, 17H), 7.07 (d, *J*=8.6, 2H), 7.03 (d, *J*=9.2, 27H), 6.87 (d, *J*=8.6, 1H), 6.80 (d, *J*=8.8, 11H), 4.83 (s, 21H), 4.78 (s, 3H), 4.68 (s, 3H), 4.16 (t, *J*=5.6, 28H), 3.05 (t, *J*=5.6, 29H); **^{13}C NMR** (100 MHz, DMSO-[d_6])) δ = 190.82 (s), 190.11 (s),189.93 (s), 172.17 (s), 166.48 (s), 166.25 (s), 164.27 (s), 163.78 (s), 160.50 (s), 140.70 (s),139.83 (s), 138.23 (s), 137.86 (s),137.23(s), 135.45 (s), 133.21 (s), 132.23 (s), 132.10 (s), 128.76 (s), 128.64 (s), 128.32 (s), 127.94 (s), 127.88 (s), 127.82 (s), 127.69 (s), 127.33 (s), 126.72 (s), 126.61 (s), 125.77 (s), 125.62 (s), 122.65 (s), 120.42 (s), 118.84 – 118.66 (m), 118.13 (s), 117.65 (s), 116.59 (s), 114.97 (s), 67.60 (s), 63.78 (s), 61.13 (s), 58.32 (s), 53.23 (s); **HRESI mass spectrum** for [**4a**]$^+$: found *m/z* 1304.4561, calcd. *m/z* 1304.4240)

Adduct 4b :

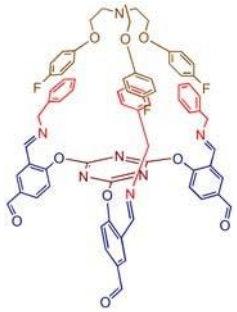

^{1}H NMR (400 MHz, DMSO-[d_6])) δ = 10.25 (s, 1H), 9.78 (s, 1H), 9.67 (s, 1H), 8.72 (s, 1H), 8.11 (s, 1H), 7.91 (s, 1H), 7.71 (d, *J*=9.9, 1H), 7.30 (d, *J*=4.1, 4H), 7.26 – 7.19 (m, 1H), 7.06 (d, *J*=8.6, 1H), 6.98 (t, *J*=8.7, 2H), 6.81 (dd, *J*=8.8, 4.3, 2H), 6.76 (d, *J*=8.8, 1H), 4.77 (s, 2H), 4.73 (s, 1H), 4.64 (s, 1H), 3.93 (t, *J*=5.7, 2H), 2.93 (t, *J*=5.7, 2H); **^{13}C NMR** (100 MHz DMSO-[d_6]) δ = 190.90 (s), 190.14 (s), 189.92 (s), 172.05 (s), 166.45 (s), 166.0 (s), 157.63 (s), 155.29 (s), 154.82 (s), 137.80 (s), 137.25 (s), 135.57 (s), 133.21 (s), 132.17 (s),128.75 (s), 127.93 (s), 127.68 (s), 125.70 (s), 122.62 (s), 120.36 (s), 118.48 (s), 116.64 (s),115.85 (s), 115.73 (s),115.65 (s), 115.63 (s), 67.10 (s), 58.43 (s), 53.61 (s);**HRESI massspectrum** for [**4b-H**]$^+$: found *m/z* 1222.6568, calcd. *m/z* 1222.4321)

Receptor 5a :

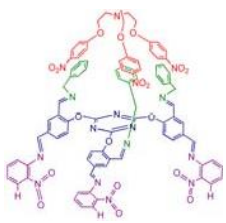

^{1}H NMR (400 MHz, DMSO-[d_6])) δ = 9.75 (s, 1H), 8.81 (s, 1H), 8.12 (d, *J*=9.2, 2H), 8.00 (d, *J*=2.1, 1H), 7.94 (dd, *J*=8.7, 1.1, 1H), 7.79 (dd, *J*=8.9, 2.1, 1H), 7.48 – 7.27 (m, 10H), 7.49 – 7.26 (m, 10H), 7.06 (d, *J*=9.2, 2H), 7.01 (d, *J*=8.1, 1H), 6.84 (d, *J*=8.8, 1H), 6.63 – 6.55 (m, 1H), 4.86 (s, 2H), 4.19 (t, *J*=5.5, 2H), 3.08 (t, *J*=5.5, 2H).

Receptor 5b :

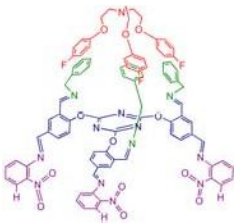

^{1}H NMR (400 MHz, DMSO-[d_6])) δ = 9.75 (s, 1H), 8.82 (s, 1H), 7.44 –7.30 (m,8H), 7.07 (t, *J*=8.8, 8H), 3H), 7.01 (d, *J*=8.5, 1H), 6.90 (dd, *J*=9.1,

4.4,2H),6.84 (d, *J*=8.8, 1H), 6.60 (t, *J*=7.7, 1H), 4.87 (s, 2H), 4.02 (t, *J*=5.8, 3H), 3.01 (t, *J*=5.8, 3H); **^{13}C NMR** (100 MHz, DMSO-[d_6]) δ = 189.94 (s), 172.20 (s), 166.47 (s), 157.61 (s), 155.27 (s), 154.82 (d, *J*=1.9), 146.21 (s), 137.88 (s), 137.24 (s), 135.69 (s), 133.22 (s), 130.32 (s), 129.48 (s), 129.14 (s), 128.76 (s), 128.64 (s), 128.33 (s), 127.94 (s), 127.89 (s), 127.83 (s), 127.70 (s), 125.62 (s), 125.38 (s), 120.44 (s), 119.18 (s), 116.59 (s), 115.86 (s), 115.74 (s), 115.65 (s), 115.63 (s), 115.47 (s), 67.11 (s), 58.32 (s), 53.59 (s).

Results and Discussion

Triazene core based ligand **1**, their corresponding adduct **2** and tripodal receptor **3**, all are highly flexible can exists in several possible conformation (confirmed through concentration dependent ^{1}H NMR (Fig. 30-38). Fig. 17 Both formyl group of each arm of ligand **1**, reacts regioselectively. Benzylamine prefer to form Schiff base with *ortho*-substituted formyl group whereas 2-nitroaniline forms Schiff base with *para*-substituted formyl group (with respect to alkoxy moiety). The concentration dependent ^{1}H NMR of adduct **2** shows five peaks corresponding to benzylic protons (Fig. 19). Upon increasing the concentration of adduct **2** to 100 mM, the number of peaks corresponding to benzylic proton (~4.8 ppm) reduced and suggest that adduct **2** exist in three major conformation in the solution state. In the presence of tripodal receptor **3**, only one peak for benzylic proton of adduct **2** remain and rest disappear to form single conformer of **4**, which later form schiff base with 2-nitroaniline to form **5**. Discrete entity **5** form dimeric capsule **5•5** in response to change in polarity of the solvent system.

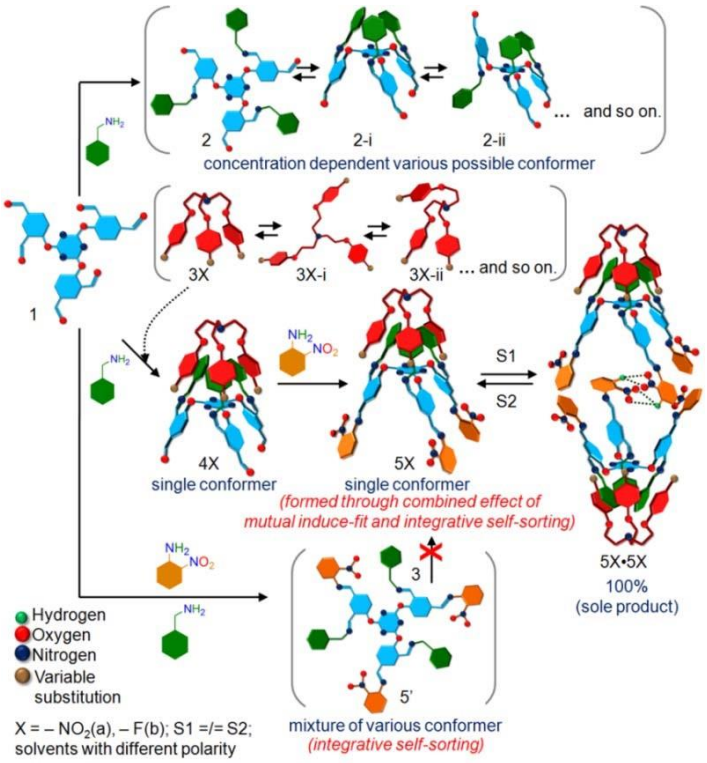

Fig. 17 Schematic presentation of the solvent polarity dependent dynamic self-assembly of receptor **5X** to hydrogen-bonded capsule **5X•5X**, effectively formed by conformer amplification of the adduct **2** with N-bridged receptor **3X** through mutual induce-fit.

Two band observed in IR spectrum for receptor **1**, one at 1666.80 cm^{-1} for *para*-substituted carbonyl group and second at 1689.21 cm^{-1} for *ortho*-substituted carbonyl group with respect to alkoxy moiety, respectively. These bands disappear in IR spectrum of the resulting complex, prepared by addition of 4.5 equivalents each of 2-nitroaniline and benzylamine, respectively (Fig. 26-29, see spectral characterization section). The biased reactivity of two unsymmetrical formyl group of receptor **1** was also observed through comparative studies of ^{1}H NMR spectra (Fig. 30 and 32). In ^{1}H NMR spectrum of receptor **1**, two well resolved peak appear at 10.33 ppm and 9.88 ppm corresponding to proton '*d*' and '*e*' respectively. After addition of benzylamine (3 equivalent), peak for proton '*d*' significantly shifted upfield and appeared at 8.80 ppm and very minor upfield shift observed for proton '*e*' and appears at 9.61 ppm. These peaks further shifted to 8.82 ppm and 9.75 ppm (for '*d*' and '*e*' protons), respectively (Fig.43) after addition of 2- nitroaniline (3 equivalents). No significant change observed in the peak position even by increasing the ratio of any component (either benzylamine or 2-nitroaniline) by five times. Positive mode of high resolution ESI mass spectrum (Fig. 18) showed expected peak cluster for the adduct **5'** in acetonitrile at *m/z* 1170.6208 ([**5'**•H_2O]$^+$, calcd. *m/z* 1170.3773).

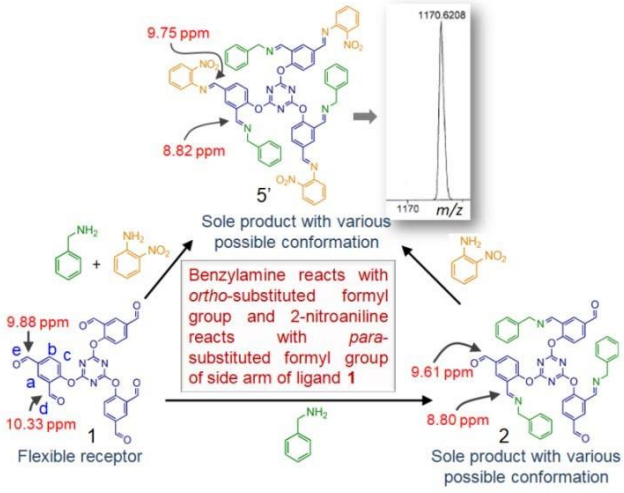

Fig. 18 Schematic representation of Schiff base **5'** formation as sole product through biased reactivity of *ortho*- and *para*-substituted formyl group (with respect to alkoxy group) of ligand **1**.

The receptor **1** and its corresponding adduct **2** are highly flexible and exist in various conformations (see Fig. 30, 33-38). A bunch of peaks appear near 4.8 ppm (for benzylic proton '*f*') in the concentration dependent ^{1}H NMR titration spectra, reveals the formation

of multiple conformer of the adduct **2** on NMR time scale (Fig. 19). The number and ratio of conformer formation is concentration dependent. At 6.25 mM concentration of receptor **1**, five peaks of equal intensity observed, indicates the formation of five different conformers. At 100 mM concentration, the number of conformers decrease to three (in 1:0.5:0.5 ratio, Fig. 31-32). Detailed studies revealed that the peak with a high intensity corresponds to the cone-shaped conformers **2-i** (Fig. 19). The decrease in the number of peaks corresponding to benzylic proton '*f*' of the adduct **2** with an increasing concentration of receptor **1** suggests that stacking of conformers **2-i** force other conformers to come in the cone-shaped conformation (almost 50% based on peak intensity).

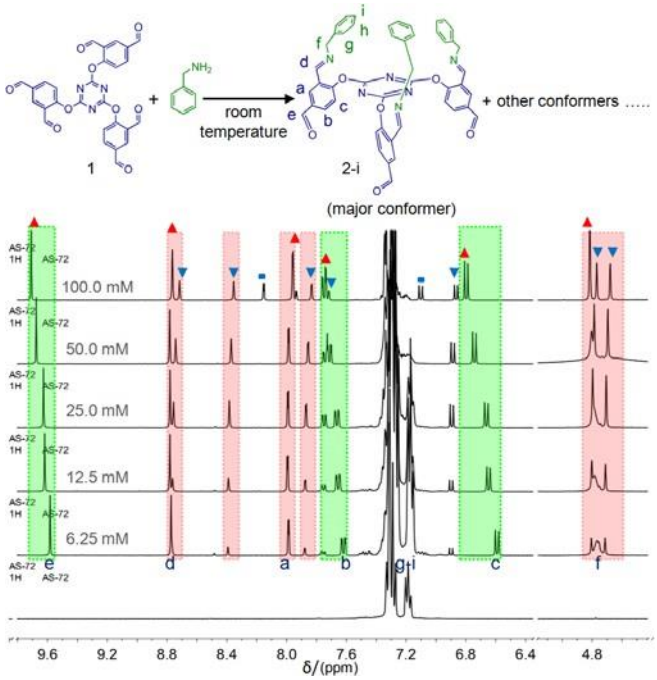

Fig. 19 Partial ^{1}H NMR titration spectra (DMSO-[d_6], 298 K) of ligand **1** in the presence of benzylamine, showing concentration dependent number and ratio of conformer formation. The triangle mark in red color shows increase in peak intensity with increase in concentration of ligand **1**. The triangle mark in blue color shows decrease in peak intensity with increase in concentration of ligand **1**. Five peak corresponding to benzylic proton appears at ~4.8 ppm at 6.25 mM of 1, suggest five different conformation of adduct **2** in the solution state. At 100 mM concentration of **1**, one major and two small peaks of equal intensity appears, suggest that at high concentration also the corresponding adduct **2** exists in different conformation.

For conformer amplification through mutual induce-fit, N-bridged C_3-symmetric receptor **3a** with electron withdrawing substituent at *para*-position of the aromatic ring

(assuming π•••π interaction will favour the process) was used. The concentration dependent ^{1}H NMR titration experiment shows that at the ratio of 1:1 of the adduct **2** and receptor **3a**, minor conformer of the adduct **2** (Fig.4) decreases significantly and major peak for benzylic proton of the adduct **2** increases from 50% to 78%. This significant change is attributed to π•••π intermolecular interactions between the aromatic ring of benzyl moiety of the adduct **2** and that of receptor **3a** through a mutual induce-fit. The absence of peak-broadening for N-bridged receptor suggest strong nature of intermolecular π•••π interactions. No change in peak position for protons corresponding to the adduct **2** and also for receptor **3a** (shown by dotted arrow, Fig. 20) observed. This observation suggest that the adduct **4a** is in a fixed conformation. The absence of new peaks near to the aliphatic protons (*a'* and *b'*) of receptor **3a** suggest that the adduct **2** is symmetrically induced (by receptor **3a**) like host-inside-host.

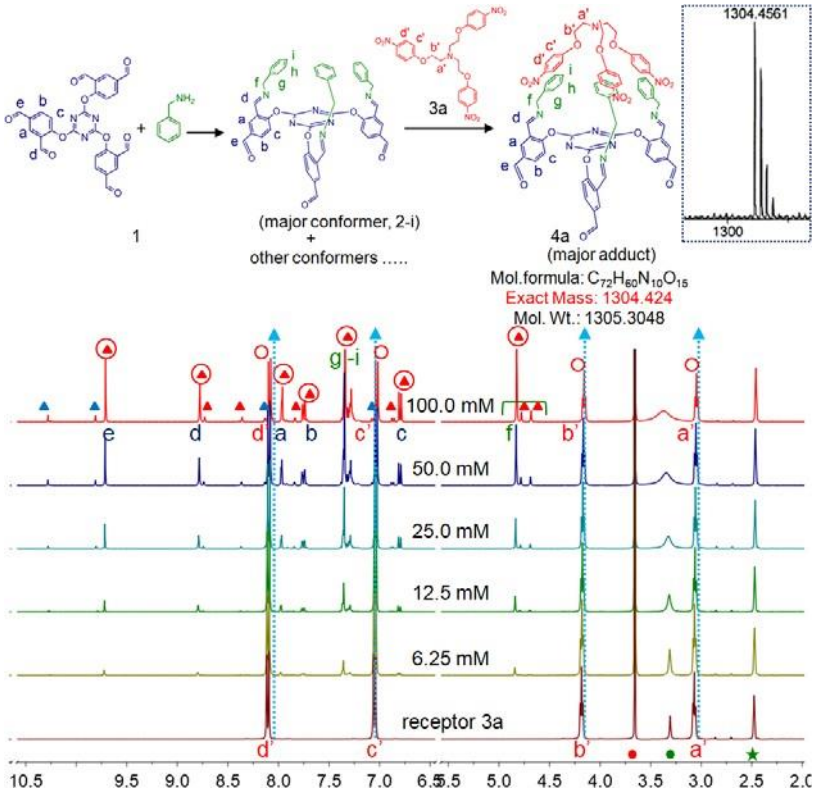

Fig. 20 Partial ^{1}H NMR titration spectra (DMSO-[d_6], 298 K) of the adduct **2** in the presence of receptor **3a** ([**3a**] = 100 mM). Red color blank circle corresponds to peak from N-bridged receptor **3a**. Triangle mark in red color inside circle shows peak corresponding to adduct **4a**, formed after mutual induced-fit. Triangle in red blue color shows residual peak from ligand **1**. Triangle in red color shows peak corresponding to other conformer of adduct **2**.

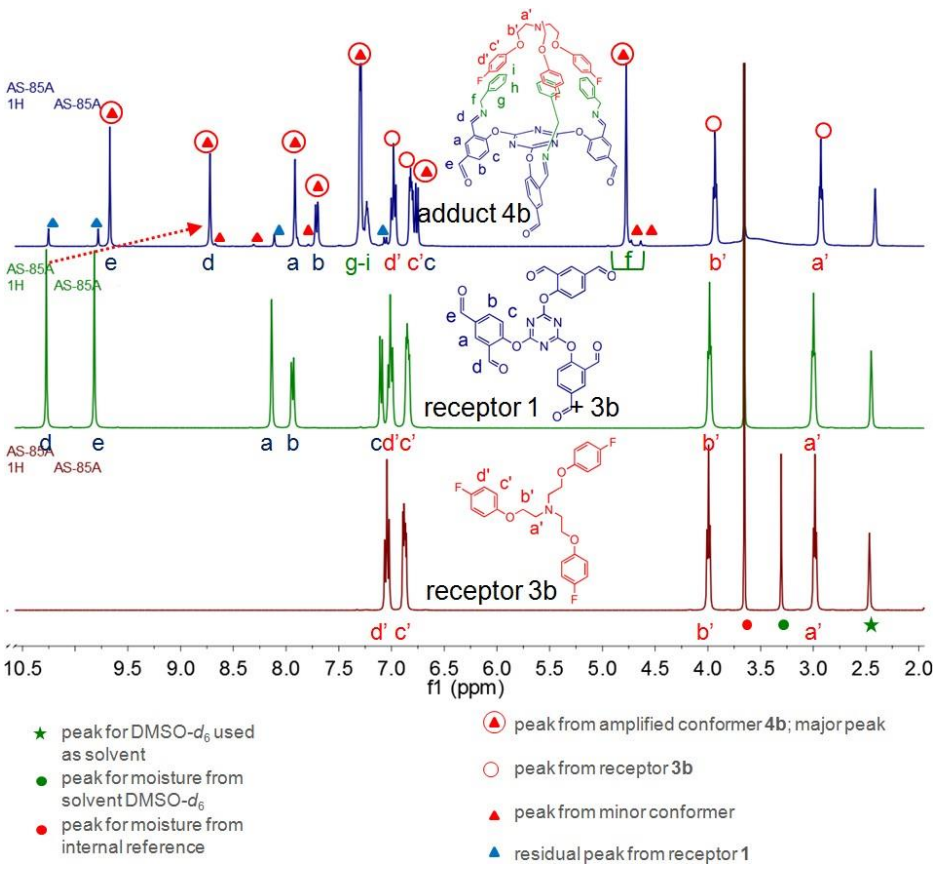

Fig. 21 ^{1}H NMR spectra (DMSO-[d_6], 298 K) of (i) receptor **3b** (*bottom*), (ii) mixture of ligand **1** and receptor **3b** (*middle*) and (iii) resultant adduct **4b**, formed after mutual induced-fit after addition of benzylamine to mixture of ligand **1** and receptor **3b** (top). Red color blank circle corresponds to peak from N-bridged receptor **3b**. Triangle mark in red color inside circle shows peak corresponding to adduct **4b**, formed after mutual induced-fit. Triangle in red blue color shows residual peak from ligand **1**. Triangle in red color shows peak corresponding to other conformer of adduct **2**.

Previously, it was shown that the size of aperture (distance between *para*-substituted group) depends upon the nature of substituent[27]. Therefore, receptor **3b** with *fluoro*- derivative of N-bridged tripodal receptor was used. Surprisingly, conformers of the adduct **2** was effectively amplified by receptor **3b** to single cone-shape conformation (adduct **4b**). An equimolar mixture solution of the adduct **2** and receptor **3b** showed almost complete suppression of the minor conformer (Fig. 21) with an amplification for major conformor **2-i** from 50% to 100%.

The discrete receptor **5b** obtained (Fig. 17) by addition of 3 equivalents of 2-nitroaniline to DMSO-[d_6] solution of the adduct **4b**. It is important to mention that the adduct **5'** was unable to transform to receptor **5b** with receptor **3b** (Fig. 17).

Probably, weak intermolecular π•••π interactions were not sufficient enough to drag the lengthy arm of receptor **5'** in a single cone-shape conformation. Even after two weeks no change was observed in the conformer amplification. Thus, effective *in-situ* formation of receptor **5b** only occur *via* adduct **4b**.

The solvent polarity dependent hydrogen bonded capsule formation through dynamic self-assembly by receptor **5b** was checked like previous report[27]. The ^{1}H NMR titration experiment was performed by adding varying concentration of $CDCl_3$ to DMSO-[d_6] solution of receptor **5b**. The upfield shift of peaks for both aliphatic and aromatic protons observed till 1:1 ratio of DMSO-[d_6] and $CDCl_3$ (*v*/*v*). This upfield shift was attributed to change in polarity of the solvent system.

Thereafter, peak for proton "*j*" of 2-nitroaniline moiety of receptor **5b** remains almost at the same position (Fig.22). while peaks for the remaining protons shifted upfield with increasing amount of $CDCl_3$, showing the formation of hydrogen bonded capsule **5b•5b**. These characteristic features were observed previously[27] for hydrogen bonded capsule formation. After partial evaporation of $CDCl_3$ from the solution mixture, resulting spectrum merges with the parent spectrum. This observation shows the reversibility of hydrogen bonded capsule formation through dynamic self-assembly[25].

In a similar experiment with the adduct **5'**, same observation noted in the peak shift but only with respect to the major conformer.This observation suggests that the formation of capsule **5'•5'** is concentration dependent (Fig. 22). Since, the concentration of the major conformer is only 50% (at 100 mM concentration), this also limits the capsule formation.

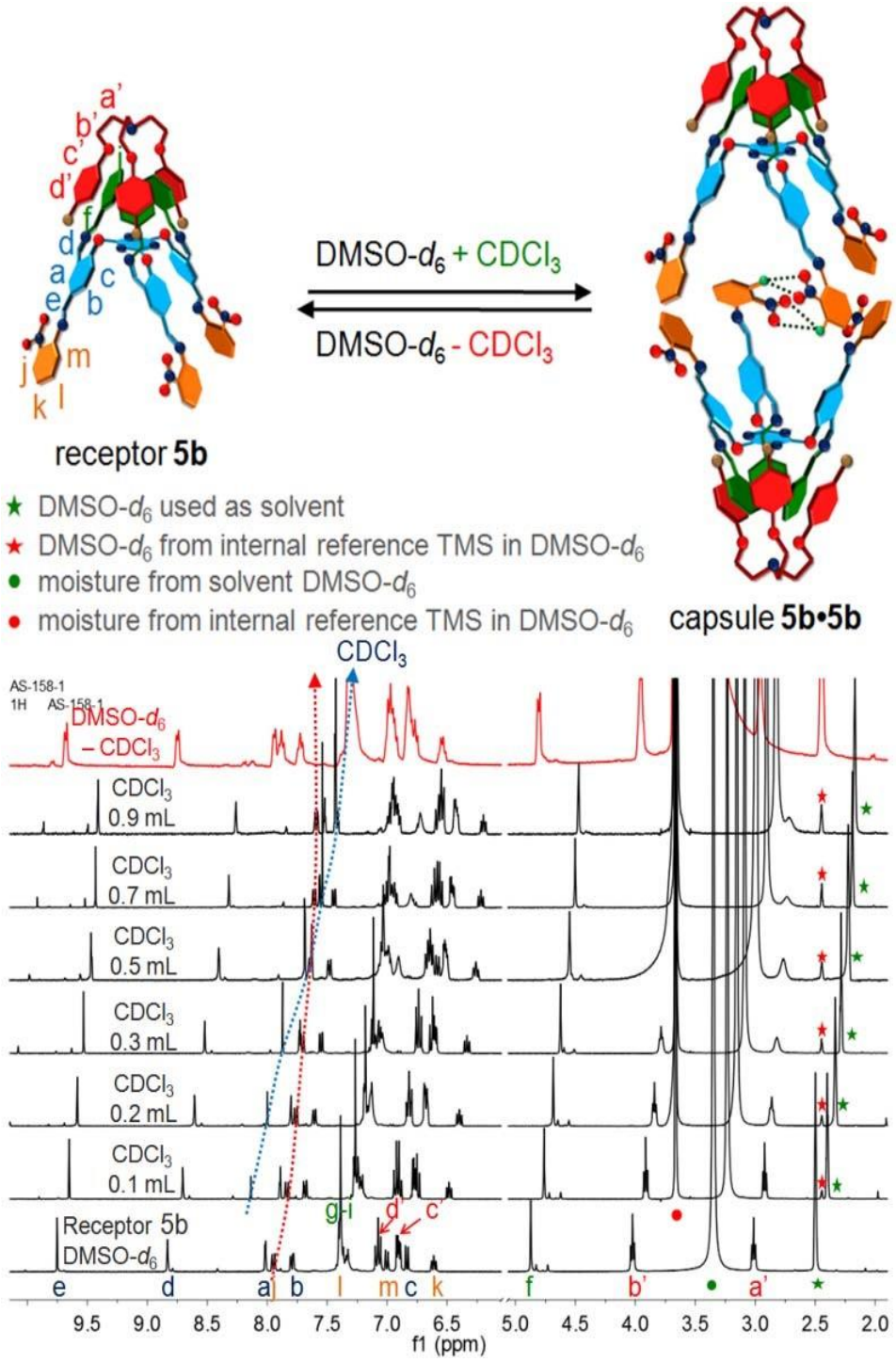

Fig. 22 Partial ^{1}H NMR titration spectra showing importance of mutual induce-fit in the solvent polarity dependent bonded capsule **5b•5b** formation (as sole product) through dynamic self-assembly.

Spectral Characterizations

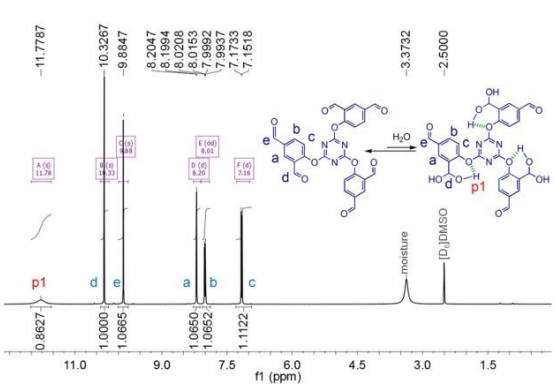

Fig. 23 ^{1}H NMR (400 MHz, DMSO-[d_6], 298K) spectrum of receptor **1**.

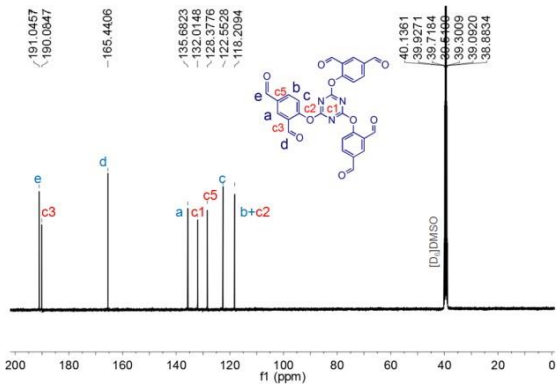

Fig. 24 ^{13}C NMR (100 MHz, DMSO-[d_6], 298K) spectrum of receptor **1**.

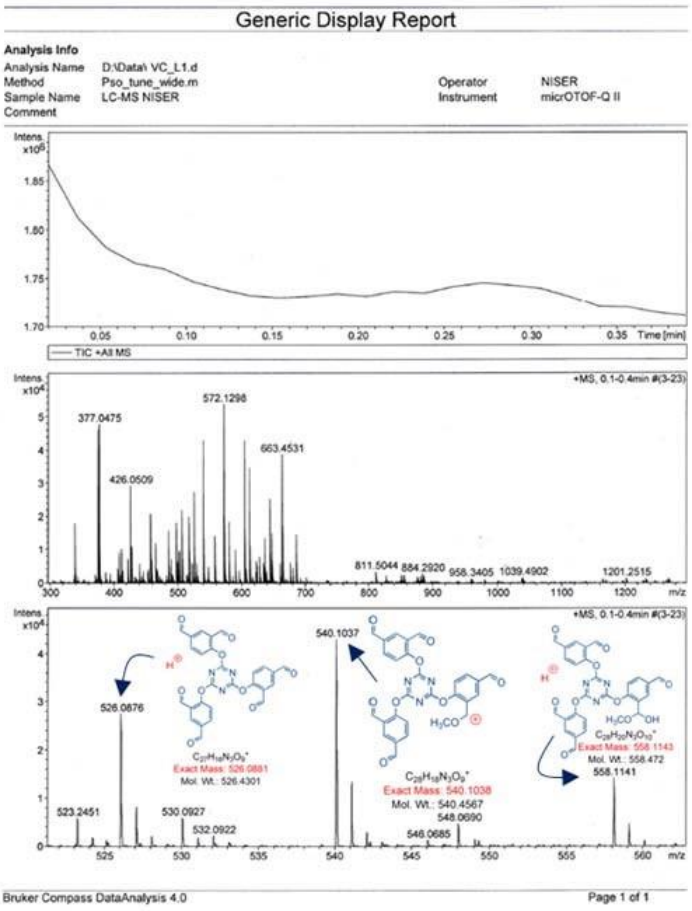

Fig. 25 HRESI mass spectrum of receptor **1** in MeOH.

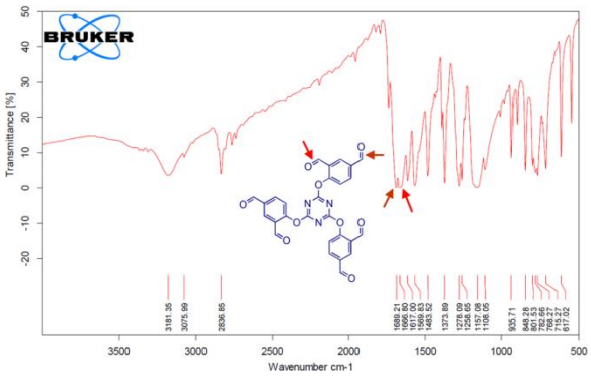

Fig. 26 IR-spectrum of receptor **1**

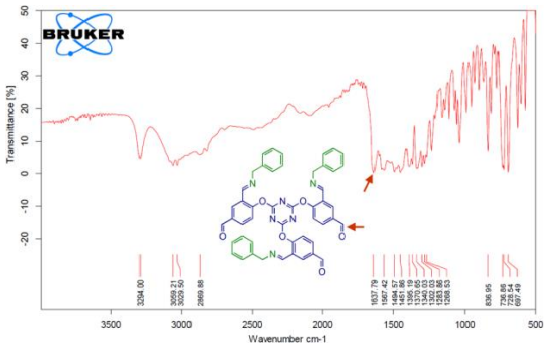

Fig. 27 IR-spectrum of mixture of receptor **1** and benzylamine.

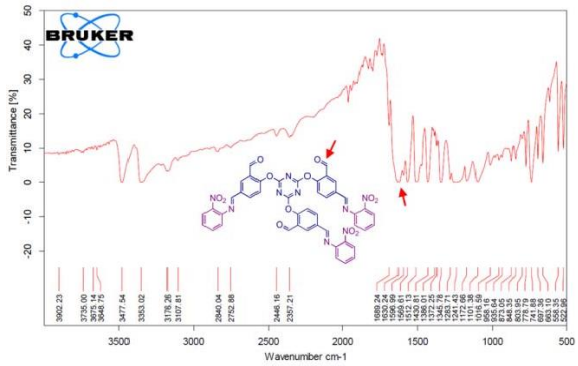

Fig. 28 IR-spectrum of mixture of receptor **1** and 2-nitroaniline with KBr pellet.

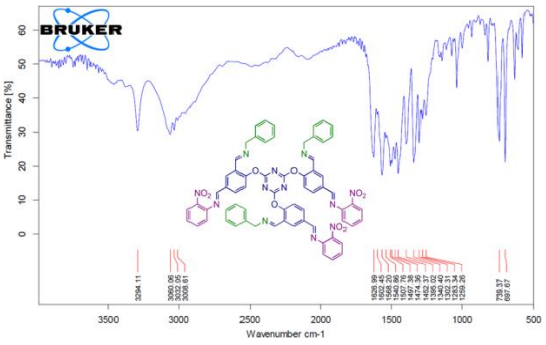

Fig. 29 IR-spectrum of mixture of receptor **1**, 2-nitroaniline and benzylamine with KBr pellet.

Flexible nature of acyclic receptors:

The flexible nature of acyclic receptor **1**, adduct **2** and N-bridged receptors **3a-3f** were shown by concentration dependent ^{1}H NMR and also by guest-dependent topology of complex in the solid-state. The concentration dependent ^{1}H NMR titration experiments were performed using internal reference TMS in DMSO-[d_6]. The peak for protons corresponding to respective receptor/adduct was shifting upfield with increase in concentration. In previous report, we have shown that in concentration dependent titration experiments, peak position for proton remains constant once the receptor come to fix conformation[1].

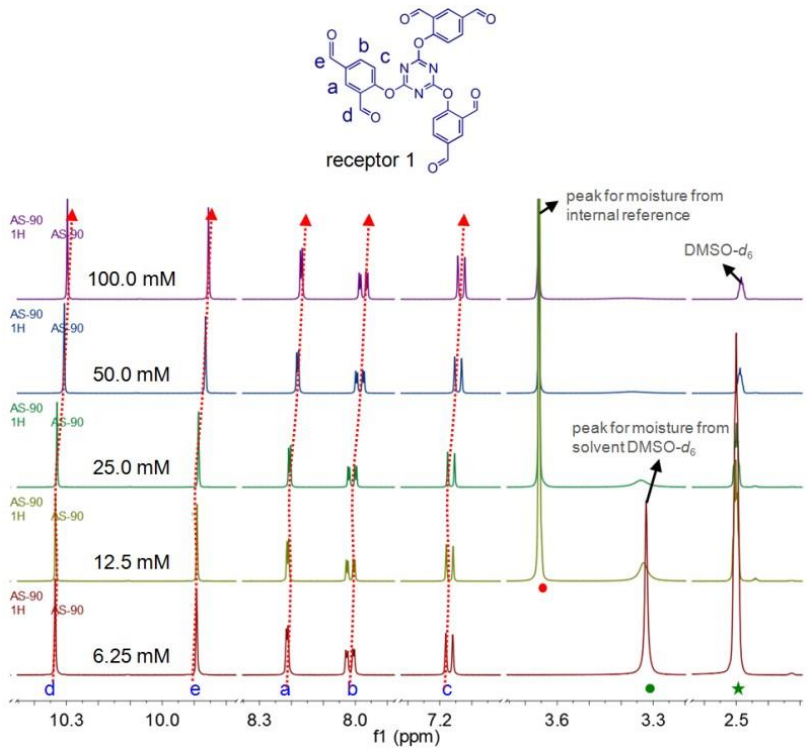

Fig. 30 Partial concentration dependent ^{1}H NMR spectra (400 MHz, [DMSO-[d_6], 298K) of receptor **1**. The upfield shift of all peaks suggest that receptor is not in the fixed conformation.

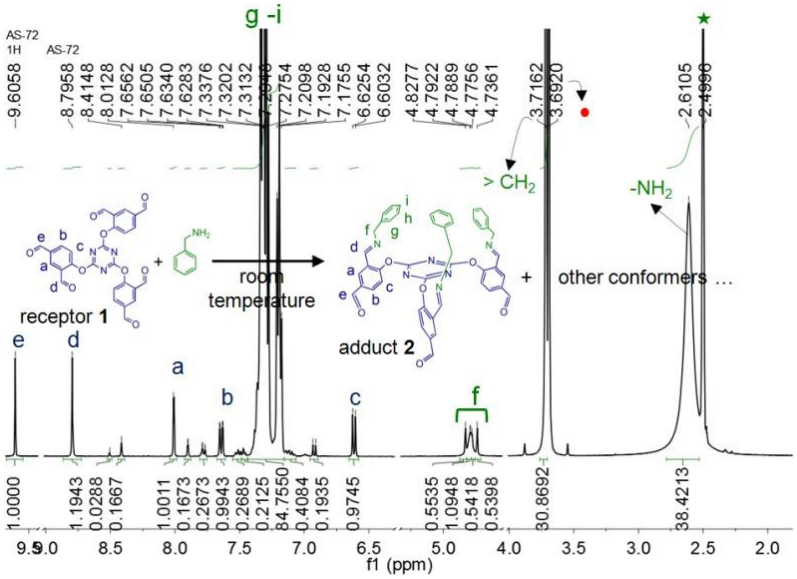

Fig. 31 Partial ^{1}H NMR spectrum (400 MHz, DMSO-[d_6], 298K) of the receptor **1** ([c] = 6.25 mM) in the presence of 100 mM of benzylamine. The five peaks corresponding to proton '*f*' of the adduct **2** (formed by Schiff's base formation of benzylamine with receptor **1**) represents for its different conformer of the adduct **2** in 1:1:1:1:1 ratio.

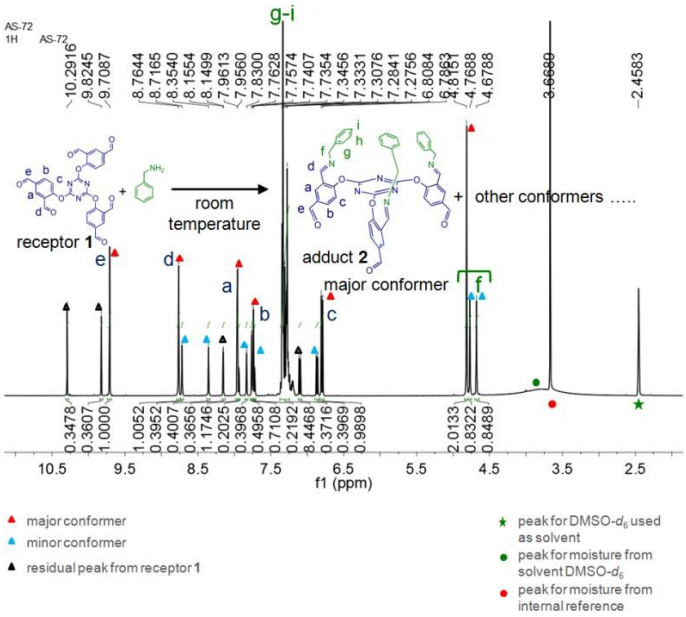

Fig. 32 Partial ^{1}H NMR spectra (400 MHz, [DMSO-[d_6], 298K) of receptor **1** ([c] = 100 mM) in the presence of 100 mM of benzylamine, to form the adduct **2**. The three peaks corresponding to proton '*f*' of the adduct **2** (formed by Schiff's base formation of benzylamine with receptor **1**) represents for its different conformer of the adduct **2** in 1:0.5:0.5 ratio. The decrease in number of conformer and increase in intensity of one conformer with increase in concentration of receptor **1** (in the presence of benzylamine) because of head-to-tail stacking of the adduct **2**.

Concentration dependent ^{1}H NMR of receptor 3a-3f

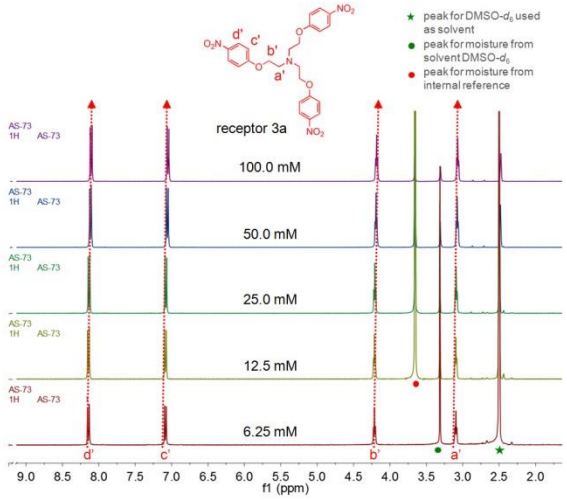

Fig. 33 Partial concentration dependent ^{1}H NMR spectra (400 MHz, DMSO-[d_6], 298K) of N-bridged receptor **3a**. The upfield shift of all peaks suggest that receptor is not in the fixed conformation.

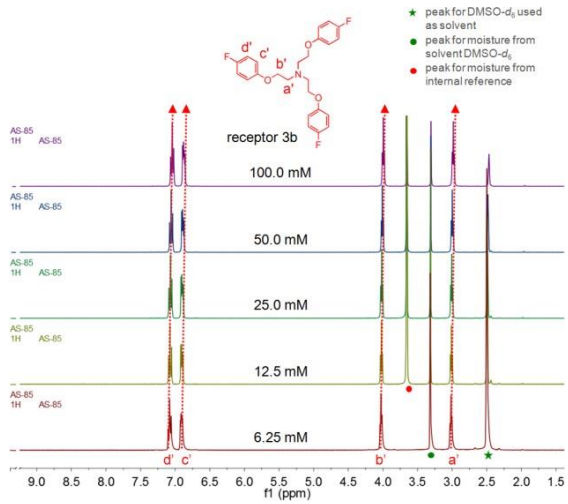

Fig. 34 Partial concentration dependent ^{1}H NMR spectra (400 MHz, DMSO-[d_6], 298K) of N-bridged receptor **3b**. The upfield shift of all peaks suggest that receptor is not in the fixed conformation.

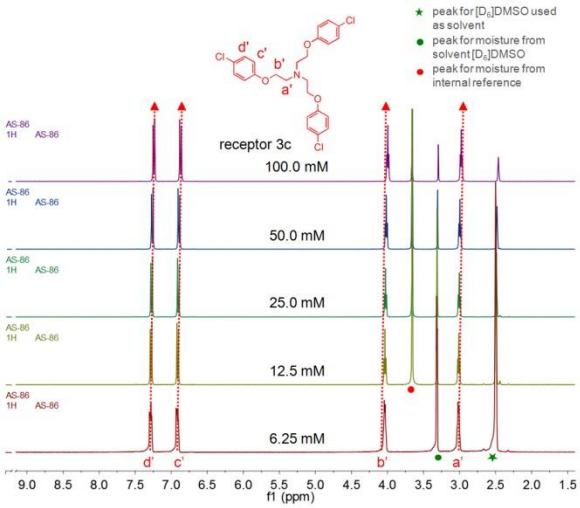

Fig. 35 Partial concentration dependent ^{1}H NMR spectra (400 MHz, DMSO-[d_6], 298K) of N-bridged receptor **3c**. The upfield shift of all peaks suggest that receptor is not in the fixed conformation.

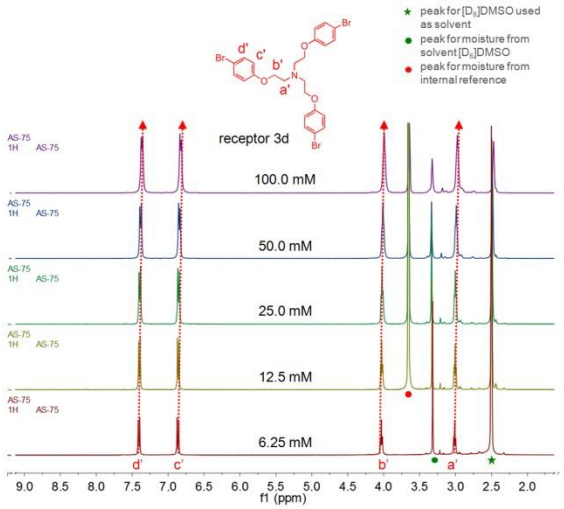

Fig. 36 Partial concentration dependent ^{1}H NMR spectra (400 MHz, DMSO-[d_6], 298K) of N-bridged receptor **3d**. The upfield shift of all peaks suggest that receptor is not in the fixed conformation.

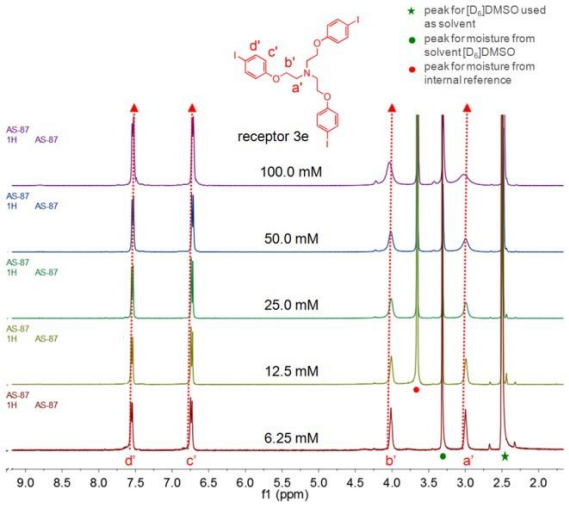

Fig. 37 Partial concentration dependent ^{1}H NMR spectra (400 MHz, DMSO-[d_6], 298K) of N-bridged receptor **3e**. The upfield shift of all peaks suggest that receptor is not in the fixed conformation.

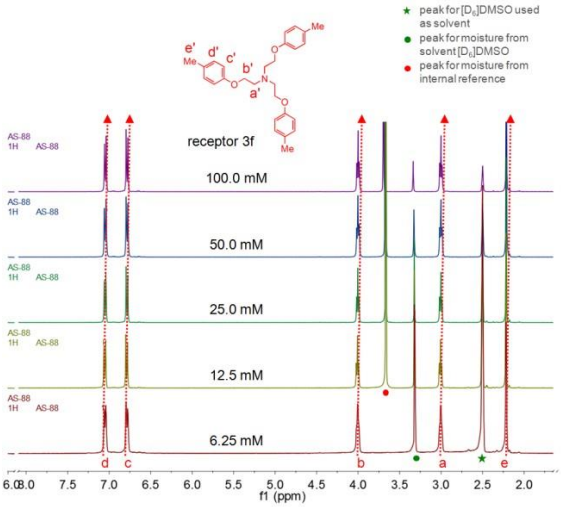

Fig. 38 Partial concentration dependent ^{1}H NMR spectra (400 MHz, DMSO-[d_6], 298K) of N-bridged receptor **3f**. The upfield shift of all peaks suggest that receptor is not in the fixed conformation.

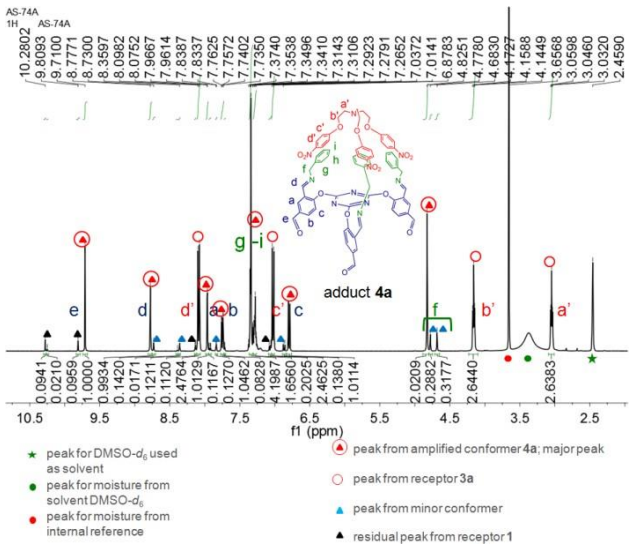

Fig. 39 ^{1}H NMR spectrum (400 MHz, DMSO-[d_6], 298K) of the adduct **4a** formed by conformer amplification of the adduct **2** by N-bridged rece ptor **3a** through mutual induce-fit.

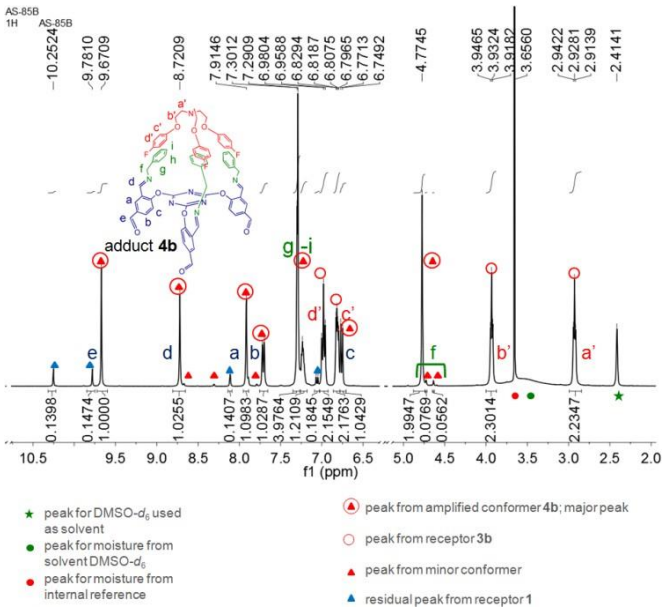

Fig. 40 ^{1}H NMR spectrum (400 MHz, DMSO-[d_6], 298K) of the adduct **4b** formed by conformer amplification of the adduct **2** by N-bridged receptor **3b**.

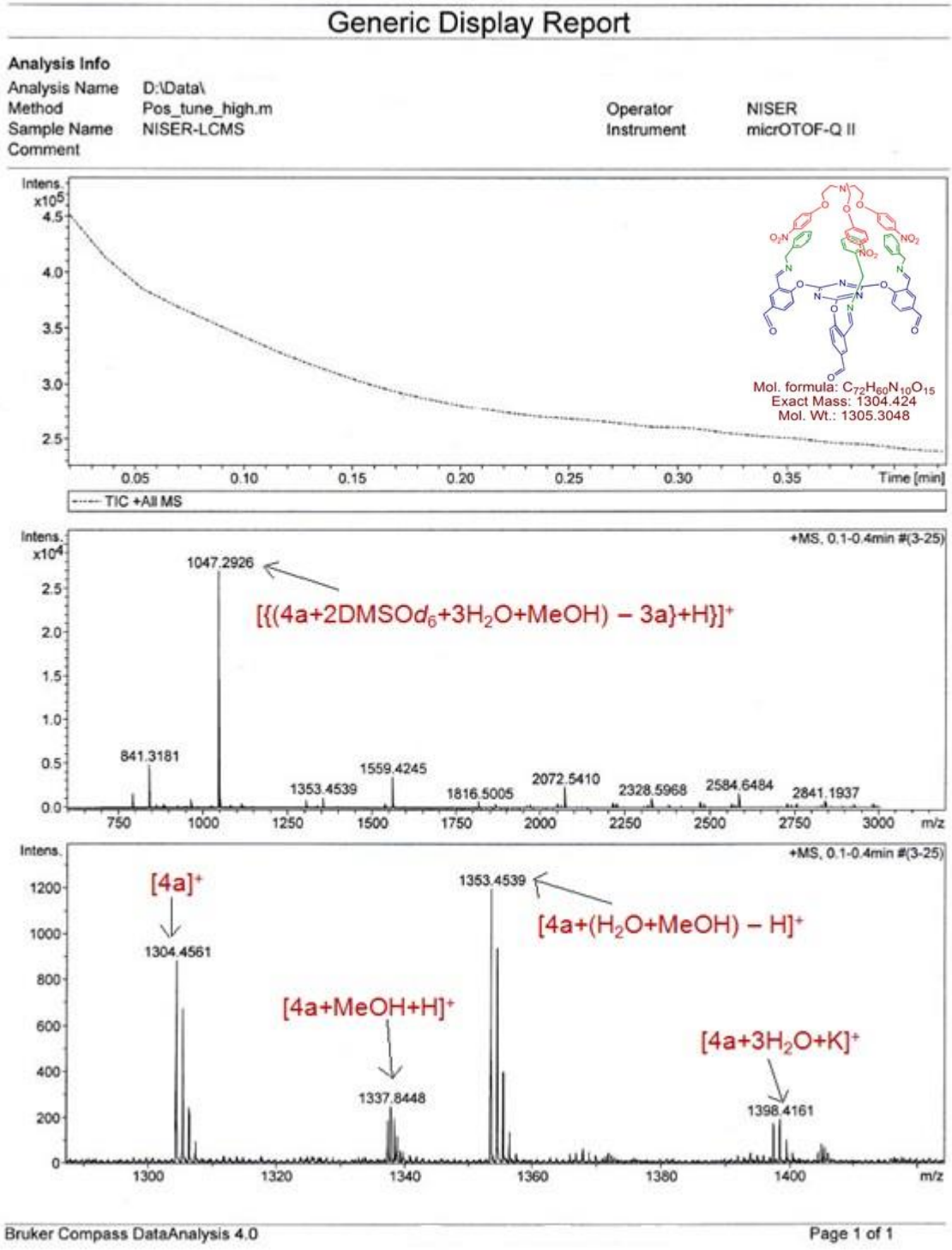

Fig. 41 HRESI mass spectrum of the adduct **4a**.

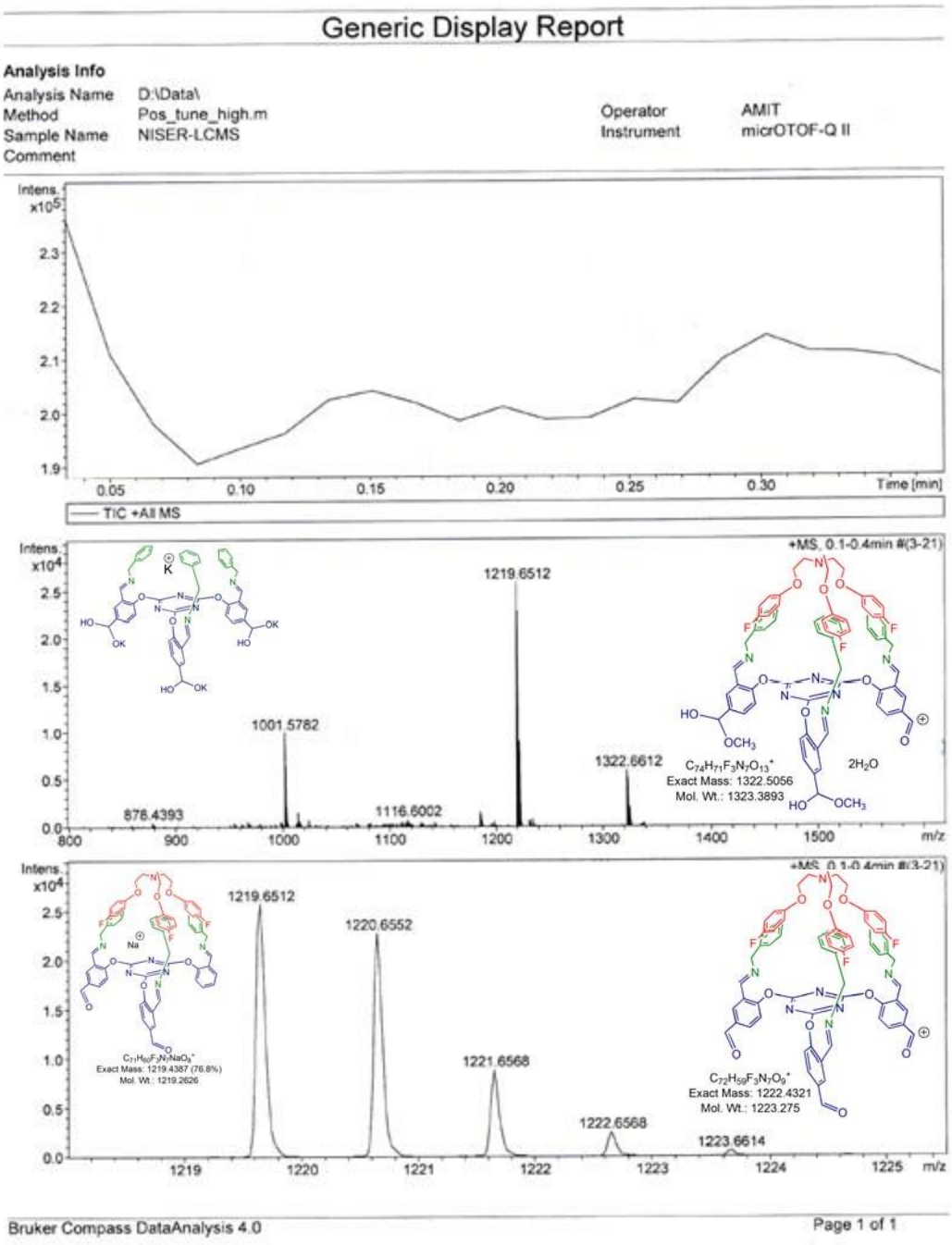

Fig. 42 HRESI mass spectrum of the adduct **4b**.

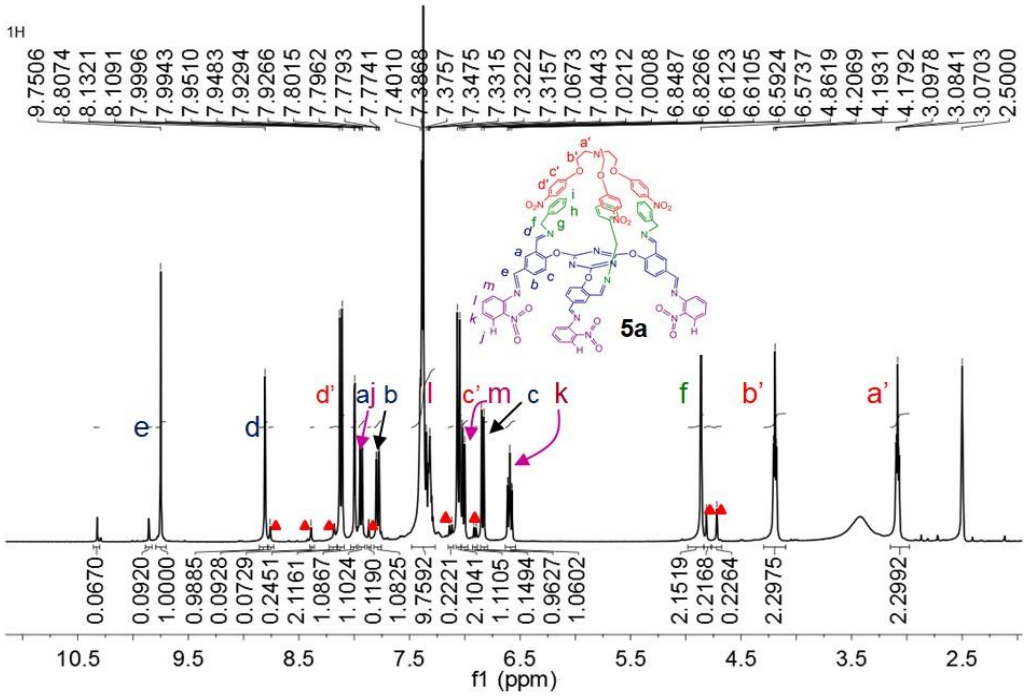

Fig. 43 ^{1}H NMR spectrum (400 MHz, DMSO-[d_6], 298 K) of receptor **5a**, prepared by adding 3 equivalents of 2-nitroaniline to the adduct **4a**. The red color triangle mark represents for peak of protons corresponding to minor conformer.

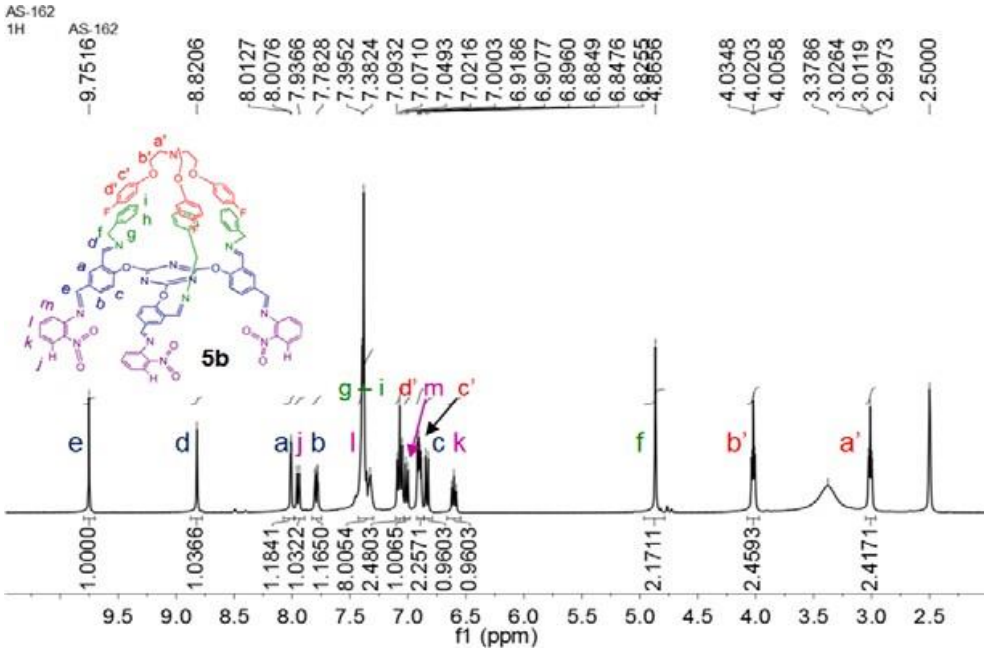

Fig. 44 ^{1}H NMR spectrum (400 MHz, DMSO-[d_6], 298 K) of receptor **5b**, prepared by adding 3 equivalents of 2-nitroaniline to the adduct **4b**.

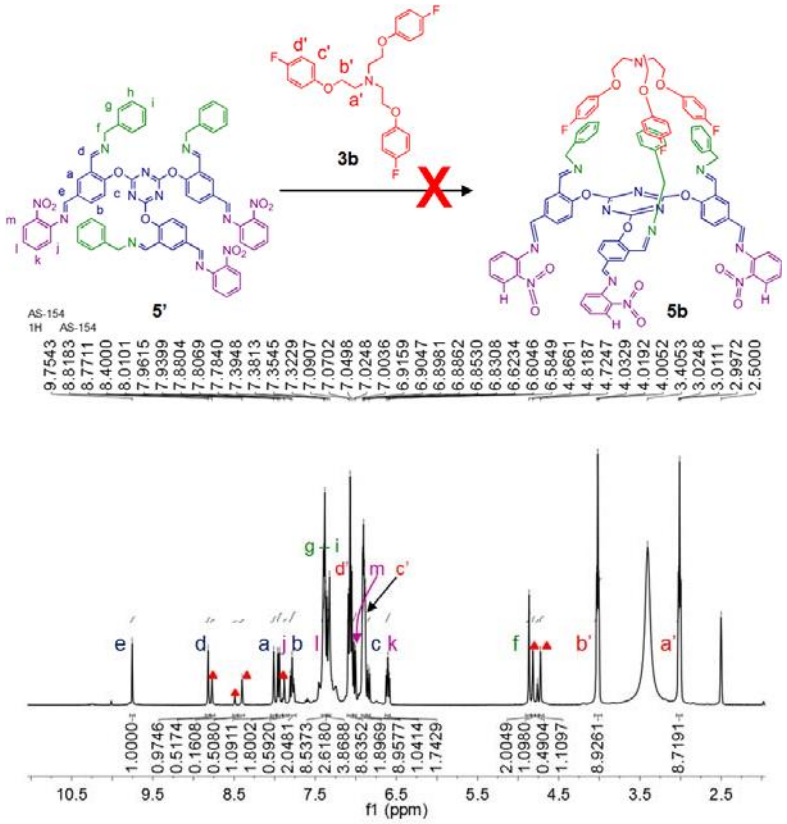

Fig. 45 ^{1}H NMR spectrum (400 MHz, DMSO-[d_6], 298 K) of sample after addition of excess (four times) amount of receptor **3b** to solution of the adduct **5'**. The spectrum showing intermolecular weak interactions from aromatic ring of the receptor **3b** was not enough to bring adduct **5'** (with lengthy arm) to single cone shape conformation like receptor **5b** even after excess (four times) addition of receptor **3b**. The red color triangle mark represents peak for protons corresponding to conformer.

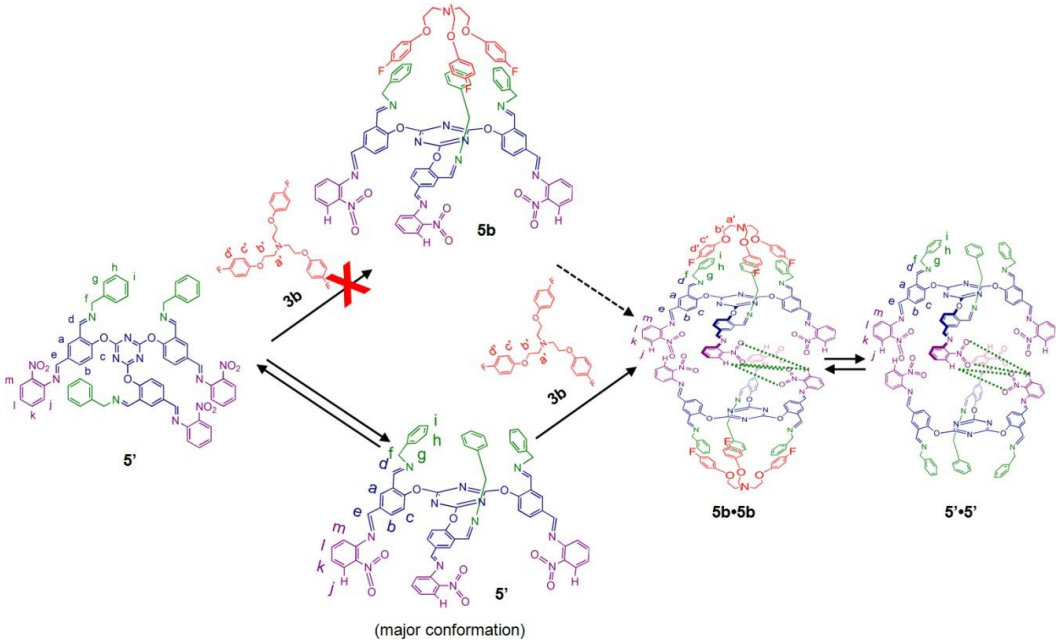

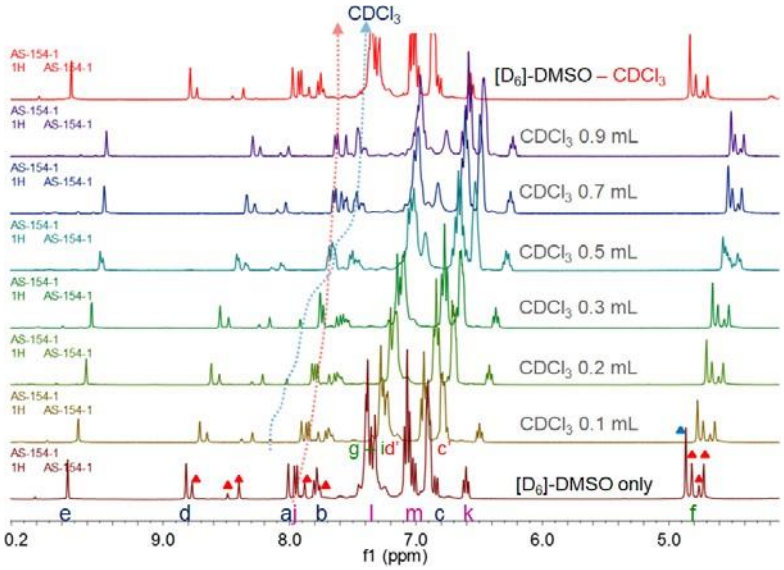

Fig. 46 The partial ^{1}H NMR titration spectra (400 MHz, 298 K) of DMSO-[d_6] solution of sample, prepared after addition of excess (four times) amount of receptor **3b** to the solution of adduct **5'**, with varying amount of $CDCl_3$. The blue and red color triangle mark represents for peak corresponding to major and minor conformer of the adduct **5'**. The spectra shows only peak "*j*" (of major conformer of adduct **5'**) shifted first upfield and then downfield, a characteristic feature of hydrogen bonded capsule formation with such system. No such changes observed for the peak corresponding to minor conformer. This observation suggest that although weak intermolecular interactions from aromatic ring of the receptor **3b** was not efficient to force minor conformer of adduct **5'** (with lengthy arm) to single cone-shape conformation like **5b** through mutual induce-fit, yet capsule formation occur *only* from major conformer of adduct **5'**.

Conclusions

In conclusion, concentration independent and effective formation of hydrogen bonded responsive capsule is reported through regioselective Schiff's base formation and mutual induce-fit. The reported capsule with π–extended arm is independent of guest molecule. The present concept can be explored further for molecular recognition, guest encapsulation/separation in response to stimuli and hopefully intrinsic driving force associated with triazene moiety (through C-H•••π and anion•••π interaction) may further facilitate to achieve the target.

References:

1. Vriezema, D. M.; Aragonès M. C.; Elemans, J. A. A. W.; Cornelissen, J. J. L. M.; Rowan, A. E.; Nolte, R. J. M. *Chem. Rev.* **2005**, *105*, 1445-1489. (b) Amouri, H.; Desmarets,C.; Moussa, J. *Chem. Rev.* **2012**, *112*, 2015-2041.
2. Steed, J. W.; Atwood, J. L. Supramolecular Chemistry, 2nd ed., Wiley, Chichester, **2009**.
3. Diederich, F. Cyclophanes, The Royal Society of Chemistry, Cambridge, **1991**.
4. Harada, A.; Takashima, Y.; Yamaguchi, H. *Chem. Soc. Rev.* **2009**, *38*, 875-882.
5. Gutsche, C. D. Calixarenes, The Royal Society of Chemistry, Cambridge, **1989**.
6. Kim, K.; Selvapalam, N.; Ko, Y. H.; Park, K. M.; Kim, D.; Kim, J. *Chem. Soc. Rev.* **2007**, *36*, 267-279.
7. (a) Cramer, F.; Saenger, W.; Spatz, H.-C. *J. Am. Chem. Soc.* **1967**, *89*, 14-20. (b) Marquez, C.; Nau, W. M. *Angew. Chem. Int. Ed.* **2001**, *40*, 3155-3160. (c) Zhang, X.; Gramlich, G.; Wang, X.; Nau, W. M. *J. Am. Chem. Soc.* **2002**, 124, 254-263. (d) Mohanty, J.; Bhasikuttan, A. C.; Nau, W. M.; Pal, H. *J. Phys. Chem. B* **2006**, *110*, 5132-5138. (e) Koner, A. L.; Nau, W. M. *Supramol. Chem.* **2007**, *19*, 55-66. (f) Pluth, M. D.; Bergman, R. G.; Raymond, K. N. *J. Am. Chem. Soc.* **2007**, *129*, 11459-11467. (g) Pluth, M. D.; Bergman, R. G.; Raymond, K. N. *Science* **2007**, *316*, 85-88. (h) Basílio, N.; Gago, S.; Parola, A. J.; Pina, F. *ACS Omega* **2017**, *2*, 70-75.
8. Wright, P. A. Microporous Framework Solids (Royal Society of Chemistry, Cambridge, **2008**).
9. (a) Qiu, S.; Zhu, G. *Coord. Chem. Rev.* **2009**, *253*, 2891-2911. (b) Kuppler, R. J.; Timmons, D. J.; Fang, Qian-Rong; Li, Jian-Rong; Makal, T. A.; Young, M. D.; Yuan, D.; Zhao, D.; Zhuang, W.; Zhou, Hong-Cai *Coord. Chem. Rev.* **2009**, *253*, 3042-3066. (c) Horcajada, P.; Gref, R.; Baati, T.; Allan, P. K.; Maurin, G.; Couvreur, P.; Férey, G.; Morris, R. E.; Serre, C. *Chem. Rev.* **2012**, *112*, 1232–1268. (d) Slater, A. G.; Cooper, A. I. *Science* **2015**, *348*, 988-1100.
10. Saleh, N.; Koner, A. L.; Nau, W. M. *Angew. Chem. Int. Ed.* **2008**, *47*, 5398-5401.
11. Singh, A.S.; Tiwari, R.K; Lee, M.M; Behera, J.N.; Sun,S.S.; Chandrashekhar,V. *Chem. Eur. J*. **2017**, *23*, 762-766
12. (a) Szaraz, S.; Oesterhelt, D.; Ormos, P. *Biophys. J.* **1994**, *67*, 1706. (b) Westheimer, F. H. *Tetrahedron* **1995**, *51*, 3. (c) Cleland, W. W.; Frey, P. A.; Cerlt, J. A. *J. Biol. Chem.* **1998**, *273*, 25529. (d) Ha, N.-C.; Kim, M.-S.; Lee, W.; Choi, K. Y.; Oh, B.-H. *J. Biol. Chem.* **2000**, *275*, 41100.
13. Yoshizawa, M.; Klosterman, J. K.; Fujita, M. *Angew. Chem. Int. Ed.* **2009**, *48*, 3418-3438.
14. (a) Kang, J.; Rebek, Jr., J. *Nature* **1997**, *385*, 50-52. (b) Schleyer, P. von R.; Manoharan, M.; Jiao, H.; Stahl, F. *Org. Lett.* **2001**, *3*, 3643-3646; (c) Cheng, M.-F.; Li, W.-K.; *Chem.*

Phys. Lett. **2003**, *368*, 630-638. (d) Kusukawa, T.; Nakai, T.; Okano, T.; Fujita, M. *Chem. Lett.* **2003**, *32*, 284-285. (e) Nishioka, Y.; Yamaguchi, T.; Yoshizawa, M.; Fujita, M. *J. Am. Chem. Soc.* **2007**, *129*, 7000-7001. (f) Klöck, C.; Dsouza, R. N.; Nau, W. M. *Org. Lett.* **2009**, *11*, 2595-2598; (g) Ghosh, S.; Isaacs, L. *J. Am. Chem. Soc.* **2010**, *132*, 4445-4454. (h) Lu, X.; Masson, E. *Org. Lett.* **2010**, *12*, 2310-2313.

15. (a) Hof, F.; Craig, S. L.; Nuckolls, C.; Rebek, Jr. J. *Angew. Chem. Int. Ed.* **2002**, *41*, 1488-1508. (b) Rebek, Jr. J. *Angew. Chem. Int. Ed.* **2005**, *44*, 2068-2078. (c) Rebek, Jr. J. *Acc. Chem. Res.* **2009**, *42*, 1660.
16. Timmerman, P.; Verboom, W.; van Veggel, F. C. J. M.; van Duynhoven, J. P. M.; Reinhoudt, D. N. *Angew. Chem. Int. Edn. Engl.* **1994**, *33*, 2345-2348.
17. Mal, P.; Breiner, B.; Rissanen, K.; Nitschke, J. R. *Science* **2009**, *324*, 1697-1699.
18. (a) Warmuth, R. *Angew. Chem. Int. Edn. Engl.* **1997**, *36*, 1347-1350. (b) Dong, Vy M.; Fiedler, D.; Carl, B.; Bergman, R. G.; Raymond K. N. *J. Am. Chem. Soc.* **2006**, *128*, 14464-14465. (c) Iwasawa, T.; Hooley, R. J.; Rebek, Jr. J. *Science* **2007**, *317*, 493-496.
19. Yoshizawa, M.; Tamura, M.; Fujita, M. *Science* **2006**, *312*, 251-254.
20. (a) Rebek, Jr. J. *Chem. Soc. Rev.* **1996**, 255-264. (b) Conn, M. M.; Rebek, Jr. J. *Chem. Rev.* **1997**, *97*, 1647-1668. (c) MacGillivary, L. R.; Atwood, J. L. *Nature* **1997**, *389*, 469-472. (d) Prins, L. J.; De Jong, F.; Timmerman, P.; Reinhoudt, D. N. *Nature* **2000**, *408*, 181-184. (e) Cohen, Y.; Evan-Salem, T.; Avram, L. *Supramol. Chem.* **2008**, *20*, 71-79. (f) Liu, Y.; Hu, C.; Comotti, A.; Ward, M. D. *Science* **2011**, *333*, 436-440.
21. (a) Grawe, T.; Schrader, T.; Gurrath, M.; Kraft, A.; Osterod, F. *Org. Lett.* **2000**, *2*, 29-32. (b) Szumna, A. *Chem. Commun*. **2009**, 4191-4193.
22. (a) Gibb, C. L. D.; Gibb, B. C. *J. Am. Chem. Soc.* **2004**, *126*, 16498. (b) Gibb, C. L. D.; Gibb, B. C. *J. Am. Chem. Soc.* **2006**, *128*, 16498. (c) Liu, S.; Gibb, B. C. *Chem. Commun.* **2008**, *32*, 3709.
23. (a) Takeda, N.; Umemoto, K.; Yamaguchi, K.; Fujita, M. *Nature* **1999**, *398*, 794-796. (b) Leininger, S.; Olenyuk, B.; Stang, P. J. *Chem. Rev.* **2000**, *100*, 853-908.
24. Scarso, A.; Borsato, G. *Supramol. Chem.* **2013**, *25*, (doi: 10.1002/9780470661345. smc079) and references therein.
25. Singh, A. S.; Sun, Shih-Sheng *Chem. Commun.* **2011**, *47*, 8563–8565.
26. Gottschalk, T.; Jaun, B.; Diederich, F. *Angew. Chem. Int. Ed.* **2007**, *46*, 260-264.
27. (a) Singh, A. S.; Sun, Shih-Sheng *Chem. Commun.* **2012**, *48*, 7392-7394. (b) Singh, A. S.; Sun, Shih-Sheng *RSC Adv.* **2012**, *2*, 9502-9510. (c) Singh, A. S.; Sun, Shih-Sheng *Chem. Commun.* **2013**, *49*, 10070-10072. (d) Singh, A. S.; Sun, Shih-Sheng *Chem. Record.* **2015**, *15*, 1021-1044.
28. (a) Cooper, A.; Nutley, M.; MacLean, E. J.; Cameron, K.; Fielding, L.; Mestres, J.; Palin, R. *Org. Biomol. Chem.* **2005**, *3*, 1863-1871. (b) Sawada, T.; Hisada, H.; Fujita, M. *J. Am. Chem. Soc.* **2014**, *136*, 4449-4451.
29. Koshland, D. E. Jr. *Angew. Chem. Int. Ed.* **1995**, *33*, 2375-2378.

30. Ringe, D.; Petsko, G. A. *Science* **2008**, *320*, 1428-1429.
31. Schmeing, T. M.; Huang, K. S.; Strobel, S. A.; Steitz, T. A. *Nature* **2005**, *438*, 520-524.
32. Koshland, D. E. Jr. *Proc. Natl. Acad. Sci.* U.S.A. **1958**, *44*, 98-104.

ORIGINALITY REPORT

15%	10%	14%	%
SIMILARITY INDEX	INTERNET SOURCES	PUBLICATIONS	STUDENT PAPERS

PRIMARY SOURCES

1	www.freepatentsonline.com Internet Source	4%
2	Ashutosh S. Singh, Shih-Sheng Sun. " Recognition, Encapsulation, and Selective Fluorescence Sensing of Nitrate Anion by Neutral -Symmetric Tripodal Podands Bearing Amide Functionality ", The Journal of Organic Chemistry, 2012 Publication	2%
3	www.faqs.org Internet Source	1%
4	Singh, Ashutosh S., and Shih-Sheng Sun. "Structurally Flexible C 3 -Symmetric Receptors for Molecular Recognition and Their Self-Assembly Properties", The Chemical Record, 2015. Publication	1%
5	Sawada, Tomohisa, Hayato Hisada, and Makoto Fujita. "Mutual Induced Fit in a Synthetic Host–Guest System", Journal of the	1%

Supervisor's Signature